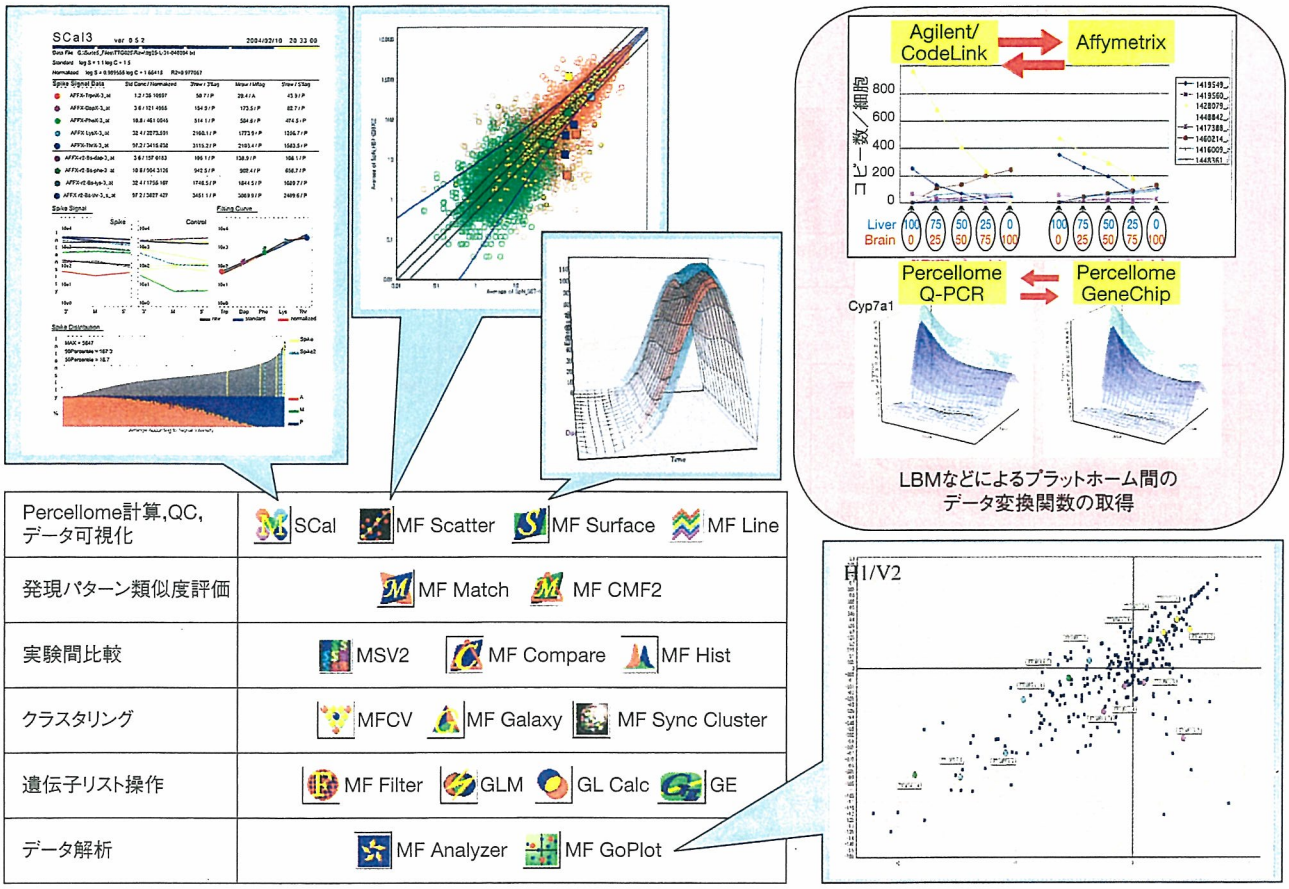

図3．3次元多層（Millefeuille）データの解析などに用いる独自開発プログラム群

品質管理とともにPrecellome計算を自動的に実施するSCal，Plotソフトウエア，3次元曲面の描画ソフト（MF Surface），など．右上はプラットホーム間のデータ変換情報の得方を示す．LBMを用いる方法（上段）と，実際の実験サンプルを用いる方法（下段）がある．いずれも，一度，両方のプラットホームでそれらのサンプルを測定する必要がある．

GeneChipとPercellome RT-PCRとの間でのコピー数の換算式がいくつかの遺伝子について得られている．この他に，Agilent社製の単色マイクロアレイとCodeLinkアレイにGSCを測定可能なカスタムアレイを用意し終え，LBMサンプルのデータなどをもとに，これらとの間の換算式も得つつある（図3右上）．

Percellome法は，Affymetrixの新しいエキソンアレイの定量性・直線性の検討にも適応可能である．Affymetrix社のHuman Exon 1.0 ST Arrayと従来型の発現アレイHuman Genome U133 plus 2について，性質の異なるヒト癌細胞株2株から調製したLBM様標準サンプル（100：0，75：25，50：50，25：75および0：100混合5サンプル）による比較を行い，両アレイ間の相関性の高いprobe setを多数検出することができた．また，既知のエキソンに対して設計されたprobe setでは発現が見られ，イントロンに対して設計されたprobe setでは発現が見られない，あるいは，既知のsplicing variantに対応したprobe setの発現が検出された，などの基本性能が確認された．しかし，Percellome法を適用して未知のsplicing variantの検出力を向上させるためには，現状では各エキソン間の定量性に問題があることが示唆された．定量値を算出する補正アルゴリズムの開発など，何らかの対策が必要であることが考えられ，現在，Affymetrix社に確認を行っている．

Ⅳ．核内受容体原性毒性のPercellomeトキシコゲノミクス解析

受容体原性毒性とは，化学物質が受容体（リガンド依存的転写因子を含む）に選択的に結合してシグナルをかく乱し，その結果生じる有害性を指す．代表例としてはダイオキシンが挙げられる．AhR（Arylhydrocarbon receptor）ノックアウトマウスでは，ダイオキシンを大量に投与しても毒性がほとんど観察されない．すなわち，野生型マウスがダイオキシンで死ぬメカニズムには，AhRが必須であり，AhRからの異常なシグナルがマウスを死に至らせていることに

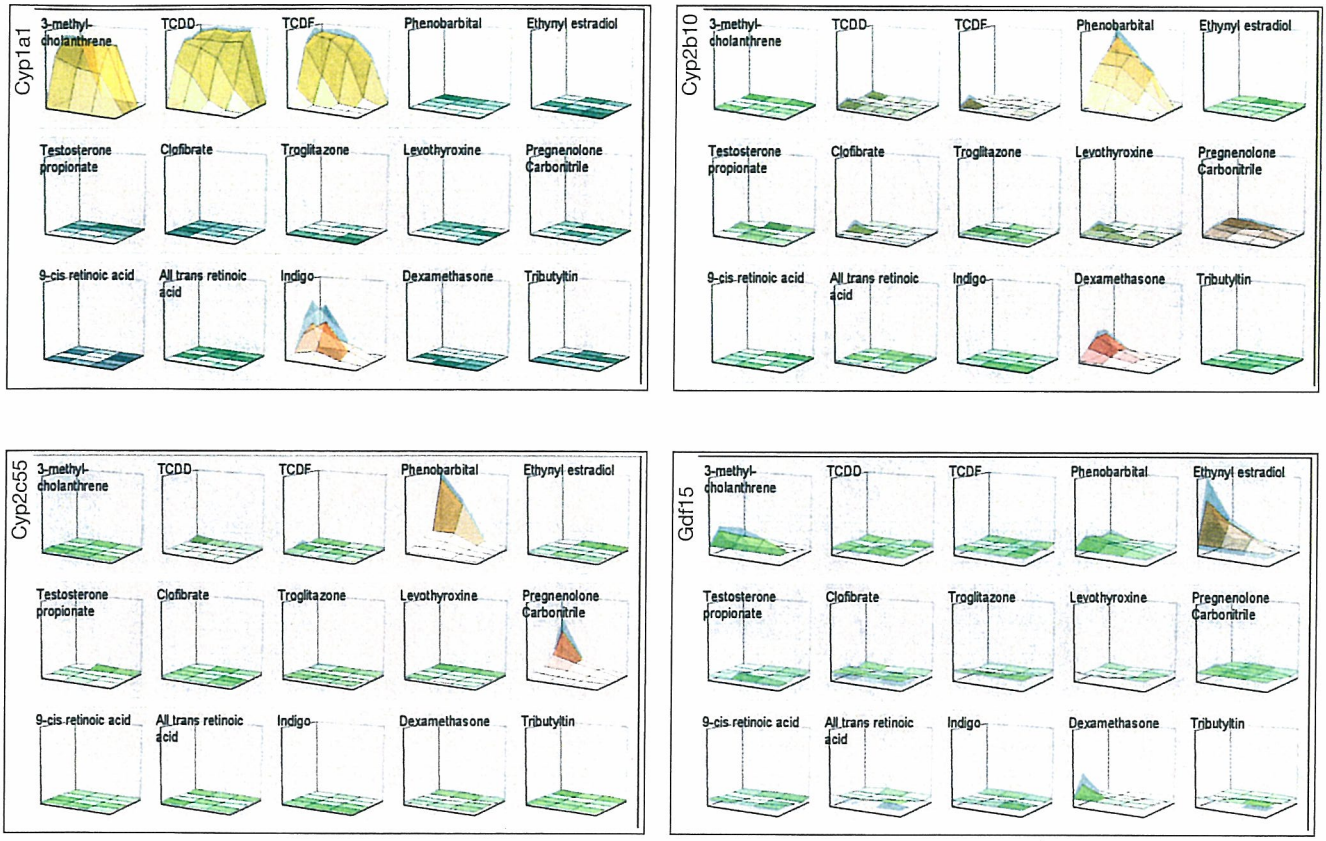

図4. 化合物間の発現比較

15種類の核内受容体リガンド化合物（各3次元グラフ内に表示）によるCyp1a1（左上），Cyp2c55（左下），Cyp2b10（右上）および，Gdf15（右下）の遺伝子発現を3次元表示したもの．各軸は，図2のとおり．縦軸のスケールは遺伝子ごとに共通．リガンドに選択的な遺伝子の発現が確認される．

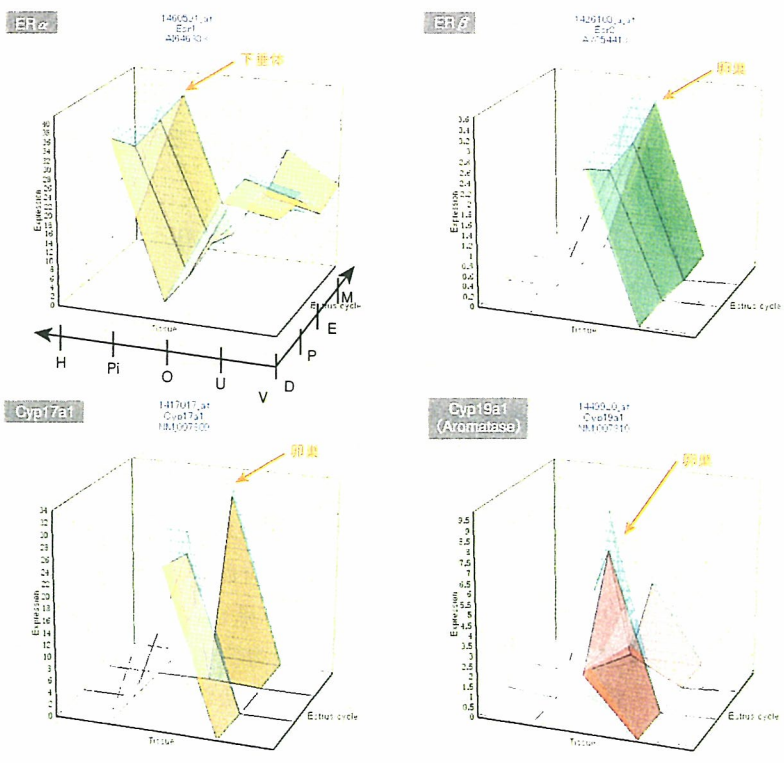

図5. 臓器間の発現比較

マウスの性周期（Diestrus，Proestrus，Estrus，Metestrusの4日間で1周期）ごとの視床下部（H），下垂体（Pi），卵巣（O），子宮（U）および膣（V）における，ERα，ERβ，Cyp17a1（steroid-17α-hydroxylase），およびCyp19a1（Aromatase）の遺伝子発現変動を3次元表示したもの．後二者の酵素は卵巣において周期性を持って発現している．

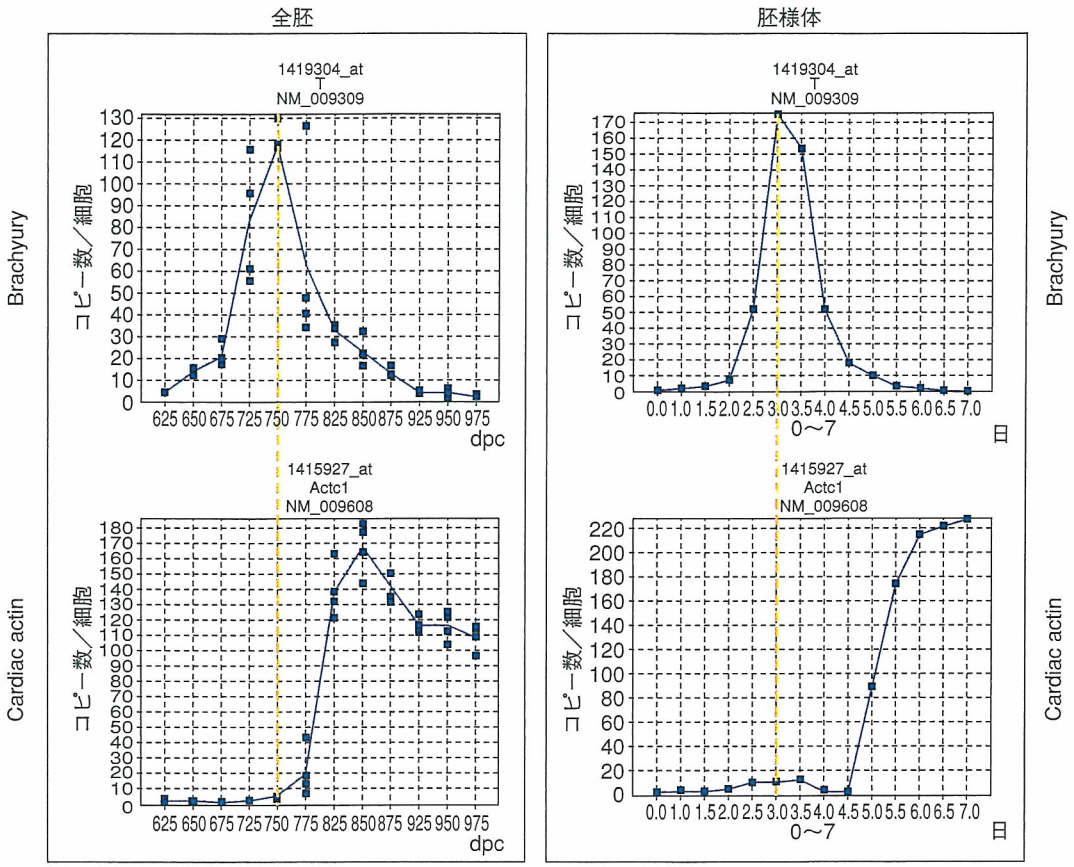

図6. マウス胎児（全胚）と胚様体の発現比較

マウス全胚の胎生6.25日～9.75日までの遺伝子発現と，胚様体の1日～7日目までの遺伝子変動の網羅的データベースから，初期中胚葉分化マーカーであるBrachyury遺伝子と，Cardiac actin遺伝子の経時変化を示す．

なる．エストロジェン活性化学物質による有害影響（内分泌かく乱化学物質問題）も同様にER（estrogen receptor）を介する受容体原性毒性と考えられ，胎生期にERを発現する組織が，低用量シグナルかく乱影響の重要標的であると考えられている．

ここでは，受容体原性毒性研究の基盤として，Percellome手法を適用して，①核内受容体作動性物質によるマウス雄肝臓の遺伝子発現変動，②性周期に伴うマウス雌生殖器遺伝子発現変動，③生後の発達過程におけるマウス雌生殖器遺伝子発現変動，の3種類のデータベースを構築した．例えば，①では10種類の核内受容体に作用する典型物質について，単回経口投与後，2，4，8，24時間目の変動を解析し，Ethynyl-estradiolがGDF15，TCDDがCyp1a1，9-cis Retinoic AcidがCyp26a1，DexamethasoneがCyp2b10，ClofibrateがCyp4a14，PCNがCyp2c55など，各々の受容体に特徴的な遺伝子発現を誘導するところがとらえられている（図4）．②の性周期データベースは視床下部，下垂体，卵巣，子宮，膣を対象としており，性周期との関連が網羅的にとらえられている（図5）．これらのデータベースは，今後，各種の候補物質が引き起こす変化を詳細に解析する際の基準として利用される．

V．発生トキシコゲノミクスへの応用

発生毒性学は，個体発生過程におけるダイナミックな遺伝子発現調節の分子機構を把握することにより，さらに正確なものに補強されると考える．現在，C57BL/6マウス胚の器官形成期初期にあたる胎生6.5～9.5日（プラグ確認日：0.5日）の，①全胚の遺伝子発現変動解析，②遺伝子欠失マウス全胚との比較，および③標的が明らかな既知発生毒性物質投与による本データベースの具体的な適用，を実施している．①についてはすでに0.25日間隔（Time point 計12点）の遺伝子発現データベースを得て，②遺伝子欠失胚のデータといくつかの注目すべき遺伝子についてはwhole mount ISHを用いた発現の検証を加えた．これと並行して，ES細胞からhanging drop法で得た胚様体の0.5日間隔の遺伝子発現データとの比較を実施している．個体発生に関与

する遺伝子群の多くは経時的に激しく変化しており，既知発生毒性物質投与実験については標的遺伝子シグナルカスケードを解析中である（図6）．

おわりに

ノーザンブロットでは実験サンプルにだけバンドが見られ，対照サンプルには遺伝子発現がないという結果を得ても，細胞1個当たりで定量してみると，対照が10コピーに対して実験サンプルが20コピーである場合がある．“無”が“有”になったのではなく，“10”が“20”になったのである．

さて，筆者らの属する毒性学でも，医学の分野でも，疾患概念や毒性概念が整理され，患者や実験動物を診断する際には，まず，そのどれに当てはまるかを検討する．すなわち，どの“典型”に近い症例であるかを検討することから始まることが多い．

しかし，最近の医学・生物学には多因子疾患・多因子形質発現制御の概念が導入され，今から何年かの後には，“21世紀初頭までは，患者の遺伝子多型を調べずして治療を行っていた時代”として，“血液型を調べずに輸血していた時代”と並び称されるようになる可能性がある．このような多因子概念が定着すると，その多くは，“有（100%）”“無（0%）”の組み合わせではなく，“70%”“50%”“90%”といった半端な数の組み合わせであることが考えられる．すなわち，今までの離散値的な“典型”例を基準とするアプローチから，連続値的な病態“スペクトラム”を直接扱うアプローチに変革していく可能性が考えられる．その際の網羅的データの解析とその蓄積の必要性を考えるとき，遺伝子発現データの定量化・標準化という問題は，今まで以上に重みを増すと考えられる．生命現象の網羅的解析にはトランスクリプトームだけでは不十分であることは自明であるが，この定量性を確保することは，これから実現されるであろう網羅的プロテオミクスなどの基盤としても重要ではないかと考える．

マイクロアレイなどから得られるトランスクリプトーム情報が，今後の医薬品審査や化学物質の安全性評価の際に必須なものとなる時代がすぐそこまで来ていることを念頭に，筆者らはPercellome法をさらに展開し，Percellome Projectデータベースを可能な限り高精度に保ちつつ毒性学的な内容を充実させるべく最大限の活動を継続して行く所存であるが，この技術，あるいは研究内容が毒性学以外の研究分野にもお役に立つことができれば幸甚である．

謝辞　本システムの開発とプロジェクトの遂行に当たっては，当毒性部の全メンバー，特に松田菜恵，辻 昌貴，森田紘一，今井あや子，安東朋子，安部麻紀，森山紀子，近藤優子，青柳千百合，相原妃佐子，渡辺 忍の各氏の卓越した働きに深謝する．本研究は厚生労働科学研究費補助金H13-生活-012，H13-生活-013，H14-トキシコ-001，H15-化学-002，H18-化学-一般-001などによる．

文献

1) Kanno J, et al: BMC Genomics (2006) 7: 64
2) 菅野 純ら: 細胞工学 (2004) 23: 685-693
3) Matsumoto S, et al: Genome Informatics (2005) 16: 183-194

毒性学

毒性の高精細解析に向けてのトキシコゲノミクス

Toxicogenomics for high-resolution toxicology

毒性学は生体と化学物質との相互作用を研究する分野であり，目的は“ヒトの安全”である．日常遭遇する化学物質(医薬品や食品を含む)が摂取された際の安全性を担保するため(毒性評価)に，実験動物の毒性所見をヒトに外挿することが行われてきた．これは実験動物もヒトも基本的に同等の生体反応を示すという前提に基づいている．そして呼吸鎖阻害，DNA損傷，活性酸素種生成など，非特異的な標的がおもな対象となってきた．これに加え，現在の分子毒性学は，生体反応メカニズムに踏み込み，受容体，転写因子などとの選択的結合によるシグナル伝達障害など標的特異性の高いものや，エピジェネティックな遅発影響などを対象とするようになり，基礎分子生物学と直結する時代に入っている．

医薬品の開発ストラテジーも標的特異性が高いものを追うものとなっており，医薬品審査行政の面からも同じことが毒性学に要求されている．そしてヒトボランティアに対するバイオ医薬品の微量投与が全員をICU送りにした最近の事件は，種差を含む分子毒性評価の重要性とその現状を示していると考えられる．また，インターネット上にはバイオ医薬品紛いの効能を謳いあげるサプリメントやダイエット/健康食品が氾濫している．これらについても場合によっては医薬品と同等の慎重さをもって評価にあたる必要がある．

胎児や子どもといった，ボランティアによる毒性評価がほとんど不可能と思われる対象のみならず，ヒトの安全のための毒性学には今後とも動物実験が必要であると考えられ，その高精度化のひとつの手段としてトキシコゲノミクスは必須であるとの認識に変わりはない．著者らは定量PCRやマイクロアレイから細胞1個当りのmRNAコピー数を得るPercellome法[1]と，そのデータ解析のためのMillefeuilleシステムを開発し，この3年間でマウス肝を中心とした約90化合物(毒性学的情報の豊富なもの)の単回曝露による初期応答遺伝子データベースを構築するとともに，シックハウス症候群を考慮した低用量域での吸入トキシコゲノミクス，発生毒性についての胎児トキシコゲノミクス，また*in situ* hybridizationによる局在確認系を立ち上げた．今後の3年間で，反復曝露による慢性毒性，および，多臓器間の関連性を検討する研究を行う．

今後の課題

トキシコゲノミクスの有効性がいまだに発揮されていないとのかんばしくない評価を耳にすることがある．しかし，著者らの経験から，それには，すくなくとも2つの解決可能な理由があると考えられる．

第1に，mRNAの変動は，思いのほか速いので，いままで以上に実験の管理を厳重にしなければ有意なデータが得られない点である．マウス肝で有意に発現する12,000(いずれかの時点で3コピー/細胞以上)の遺伝子のうち，概日変動を示す遺伝子が3,600以上あり，激しい遺伝子では数十倍以上の発現差がみられる．まず，動物飼育施設の明暗サイクルを2週間以上一定に保ちマウスの概日リズムを安定化する．そのうえで，マウスに検体を投与する時刻，および，サンプルを採取する時刻を±30分以内に限定することではじめて正確なデータが得られる．肺や腎も同様の注意が必要である．第2に，蛋白，とくにリン酸化をはじめとする蛋白合成を伴わない早い反応とのリンケージが取れないとの指摘である．この問題点についてもPercellome法を用いた高精度解析によって間接的ながら解決策を提供できることが示されつつある．すなわち，リン酸化により制御される転写因子の働きが，時間差はあるものの，その遺伝子発現の変動として捕捉されている．

おわりに

従来の毒性学に対してのトキシコゲノミクスは，たとえ話としては光学顕微鏡に対しての電子顕微鏡のような立場にある．すなわち，より高精度な情報を得る手段であるため，いままでの実験設計と精度では不十分な場合がある．そして真の実用化には“新しい教科書”を書く時間が必要であることも事実である．一方で，電子顕微鏡と異なるのは網羅的かつ膨大なデジタル情報が得られる点であり，インフォマティクスの助けが必須な理由である[2]．分子毒性学の実用化のために，トランスクリプトームデータを相互に直接比較できるPercellome法の特徴を生かしたコンソーシアムの構築をめざし，共同研究を含めたさまざま生体反応研究を進めているところである．臨床の最先端から分子生物学の最先端まで連携をさらに広げる際のひとつのきっかけとなれば幸甚である．

(厚労科研費 H13-生活-012, H13-生活-013, H14-トキシコー 001 および H15-化学-002)

1) Kanno, J. et al.：“Per cell” normalization method for mRNA measurement by quantitative PCR and microarrays. *BMC Genomics*, **7**：64, 2006.
2) Matsumoto, S. et al.：Mass Distributed Clustering：A New Algorithm For Repeated Meas-

urements in Gene Expression Data. *Genome Informatics*, **16** (2)：183-194, 2005.

菅野　純／Jun KANNO
国立医薬品食品衛生研究所・安全性生物試験研究センター毒性部

膠原病学

顕微鏡的多発血管炎と*KIR*多型

Genetic interaction between killer cell immunoglobulin-like receptor (KIR) and HLA genes with microscopic polyangiitis (MPA)

Killer cell immunoglobulin-like receptor (KIR) は NK 細胞や一部の T 細胞に発現する活性化型・抑制型分子群である．活性化型 KIR のリガンドは不明であるが，抑制型 KIR のいくつかは HLA-class I 分子をリガンドとして認識することが知られている．*KIR* 遺伝子ファミリーはヒト染色体 19q13.4 上の leukocyte receptor complex (LRC) 内に位置し，各遺伝子座における塩基多型のみならず，ハプロタイプ上の遺伝子座の数の多型 (copy number polymorphism) が存在する[1]．さらに，リガンドである HLA も高度に多型的であるが，それぞれが別の染色体上に存在し，独立に遺伝することから，個体における KIR と HLA の組合せは多様であり，これが免疫応答の個体差に関連する可能性が推測されている．

*KIR*多型の関連研究

これまでにいくつかの自己免疫疾患やウイルス感染症の関連研究において，*KIR* 遺伝子多型との関連を示す報告がある[2]．アメリカ人集団において血管炎を合併した関節リウマチや，乾癬性関節炎などの自己免疫疾患では *KIR2DS1*，*KIR2DS2* など活性化型 *KIR* 遺伝子が患者群において高い頻度で観察されている．また，AIDS の進行が遅いタイプの *KIR* 遺伝子型や，C 型肝炎ウイルスのクリアランスにかかわる *KIR-HLA* 遺伝子型の組合せなど，ウイルス感染症の臨床経過との関連も報告されている．

*KIR*多型と顕微鏡的多発血管炎

顕微鏡的多発血管炎 (MPA) は急速進行性腎炎や肺出血などの臓器障害を伴う稀少疾患であり，抗好中球細胞質抗体 (ANCA) 産生によって特徴づけられる．患者は高齢者に多く，病因はよく知られていないが，ウイルスや細菌感染との関連を示唆する報告もある．当研究室ではこれまでに日本人 MPA において，*HLA-DRB1*＊*0901-DQB1*＊*0303* ハプロタイプが有意に増加していることを報告している[3]．

今回，著者らは，日本人集団における *HLA*，*KIR* 遺伝子群と MPA の疾患感受性の検討を目的とした多施設共同研究を行った[4]．日本人 MPA 43 例，健常対照者 239 例の末梢血中のゲノム DNA を用いて *HLA-B* と *HLA-C* を決定し，*KIR* の 14 遺伝子座を PCR-SSP 法によりタイピングして，それぞれ単独で疾患との関連を検討するとともに，*KIR* と *HLA* の遺伝子型の組合せと MPA の疾患感受性との関連を検討した．

HLA 単独では MPA と健常群に統計学的に有意な差はみられなかった一方，*KIR* に関しては活性化型受容体遺伝子である *KIR2DS3* の陽性率が健常群の 16.7% に比べ MPA では 4.7% と有

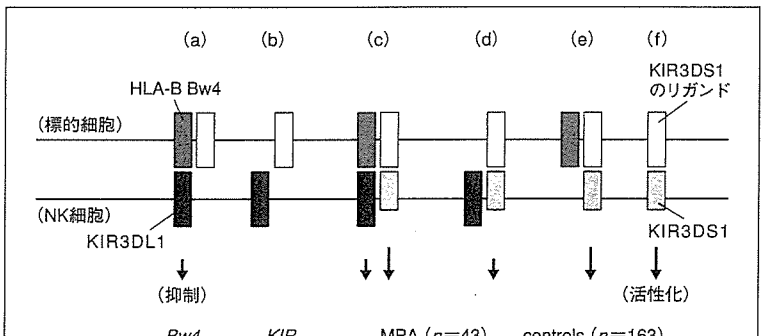

	Bw4	*KIR*	MPA (*n*=43)	controls (*n*=163)
(a)	+	*3DL1+/3DS1−*	20 (46.5%)*	44 (27.0%)
(b)	−	*3DL1+/3DS1−*	8 (18.6%)	39 (23.9%)
(c)	+	*3DL1+/3DS1+*	6 (14.0%)	38 (23.3%)
(d)	−	*3DL1+/3DS1+*	9 (20.9%)	33 (20.2%)
(e)	+	*3DL1−/3DS1+*	0 (0.0%)	7 (4.3%)
(f)	−	*3DL1−/3DS1+*	0 (0.0%)	2 (1.2%)

図 1　MPAおよび健常群における*HLA-B Bw4*と*KIR3DL1/3DS1*の組合せ

KIR3DL1 は HLA-B アリルのうち約半数に存在する Bw4 エピトープを有するアリル産物に反応する．KIR3DS1 と HLA-B との反応は証明されていないため，ここでは未知のリガンドが存在すると仮定して示してあるが，*KIR3DS1* は *KIR3DL1* 遺伝子座における活性化型アリルであり，細胞外ドメインの相同性から何らかの条件下で Bw4 と反応する可能性が指摘されている．*HLA-B Bw4* と *KIR3DL1/3DS1* それぞれの遺伝子型の組合せは 6 通りに分類されるが，これらのうちで機能的にもっとも抑制的であると予想される *HLA-B Bw4* 陽性・*KIR3DL1* 陽性・*KIR3DS1* 陰性という群 (a) が MPA において 46.5% と対照群の 27.0% と比較してオッズ比 2.35 で有意に増加していた．
*p=0.014 (χ^2test)，OR=2.35，95%CI：1.18-4.70

Premature ovarian failure in androgen receptor-deficient mice

Hiroko Shiina*†‡, Takahiro Matsumoto*‡§, Takashi Sato*, Katsuhide Igarashi¶, Junko Miyamoto*, Sayuri Takemasa*, Matomo Sakari*§, Ichiro Takada*, Takashi Nakamura*§, Daniel Metzger‖, Pierre Chambon‖, Jun Kanno¶, Hiroyuki Yoshikawa†, and Shigeaki Kato*§**

*Institute of Molecular and Cellular Biosciences, University of Tokyo, 1-1-1 Yayoi, Bunkyo-ku, Tokyo 113-0032, Japan; §Exploratory Research for Advanced Technology, Japan Science and Technology, 4-1-8 Honcho, Kawaguchi, Saitama 332-0012, Japan; †Department of Obstetrics and Gynecology, Institute of Clinical Medicine, University of Tsukuba, 1-1-1 Tennoudai, Tsukuba, Ibaraki 305-8575, Japan; ¶Division of Cellular and Molecular Toxicology, National Institute of Health Sciences, 1-18-1 Kamiyoga, Setagaya-ku, Tokyo 158-8501, Japan; and ‖Institut de Genetique et de Biologie Moleculaire et Cellulaire, Centre National de la Recherche Scientifique, Institut National de la Santé et de la Recherche Médicale, Universite Louis Pasteur, College de France, 67404 Illkirch, Strasbourg, France

Edited by Bert W. O'Malley, Baylor College of Medicine, Houston, TX, and approved November 10, 2005 (received for review August 5, 2005)

Premature ovarian failure (POF) syndrome, an early decline of ovarian function in women, is frequently associated with X chromosome abnormalities ranging from various Xq deletions to complete loss of one of the X chromosomes. However, the genetic locus responsible for the POF remains unknown, and no candidate gene has been identified. Using the Cre/LoxP system, we have disrupted the mouse X chromosome androgen receptor (*Ar*) gene. Female $AR^{-/-}$ mice appeared normal but developed the POF phenotype with aberrant ovarian gene expression. Eight-week-old female $AR^{-/-}$ mice are fertile, but they have lower follicle numbers and impaired mammary development, and they produce only half of the normal number of pups per litter. Forty-week-old $AR^{-/-}$ mice are infertile because of complete loss of follicles. Genome-wide microarray analysis of mRNA from $AR^{-/-}$ ovaries revealed that a number of major regulators of folliculogenesis were under transcriptional control by AR. Our findings suggest that AR function is required for normal female reproduction, particularly folliculogenesis, and that AR is a potential therapeutic target in POF syndrome.

male hormone | nuclear receptor | female physiology | folliculogenesis | kit ligand

Premature ovarian failure (POF) is defined as an early decline of ovarian function after seemingly normal folliculogenesis (1). Genetic causes of POF have been frequently associated with X chromosome abnormalities (1, 2). Complete loss of one of the X chromosomes, as in Turner syndrome, and various Xq deletions are commonly identified as a cause of POF. However, responsible X-linked genes and their downstream targets have not been identified so far.

The androgen receptor (*Ar*) gene, which is the only sex hormone receptor gene on the X chromosome, is well known to be essential not only for the male reproductive system, but also for male physiology. In contrast, androgens are considered as male hormones; therefore, little is known about androgens' actions in female physiology, although AR expression in growing follicles has been described (3). However, because excessive androgen production in polycystic ovary syndrome causes infertility with abnormal menstrual cycles (4, 5), it is possible that AR-mediated androgen signaling also plays an important physiological role in the female reproductive system. Recently, using Cre/LoxP system, we generated an AR-null mutant mouse line (6) and demonstrated that inactivation of AR resulted in arrest of testicular development and spermatogenesis, impaired brain masculinization, high-turnover osteopenia, and late onset of obesity in males (7–9). At the same time, no overt physical or growth abnormalities were observed in female $AR^{-/-}$ mice. Therefore, to further examine potential role of AR in female physiology, we characterized female reproductive system in $AR^{-/-}$ females. Herein we show that female $AR^{-/-}$ mice develop the POF phenotype. At 3 weeks of age, $AR^{-/-}$ females had apparently normal ovaries with numbers of follicles similar to those in the wild-type females. However, thereafter the number of healthy follicles in the $AR^{-/-}$ ovary gradually declined, with a marked increase of atretic follicles, and by 40 weeks $AR^{-/-}$ mice became infertile, with no follicle detectable in the ovary. Reflecting this age-dependent progression in ovarian abnormality, several genes known to be involved in the oocyte–granulosa cell regulatory loop were identified by microarray analysis as AR downstream target genes. These findings clearly demonstrate that AR-mediated androgen signaling is indispensable for the maintenance of folliculogenesis and implicate impaired androgen signaling as a potential cause of the POF syndrome.

Materials and Methods

Generation of AR Knockout Mice. *AR* genomic clones were isolated from a TT2 embryonic stem cell genomic library by using human *AR* A/B domain cDNA as a probe (6). The targeting vector consisted of a 7.6-kb 5′ region containing exon 1, a 1.3-kb 3′ homologous region, a single loxP site, and a neo cassette with two loxP sites (10). Targeted clones (FB-18 and FC-61) were aggregated with single eight-cell embryos from CD-1 mice (11, 12). Floxed *AR* mice (C57BL/6) were then crossed with CMV-Cre transgenic mice (6). The two lines exhibited the same phenotypic abnormalities. The chromosomal sex of each pup was determined by genomic PCR amplification of the Y chromosome *Sry* gene (13).

Western Blot Analysis. To detect AR protein expression, ovarian cell lysates were separated by SDS/PAGE and transferred onto nitrocellulose membranes (14). Membranes were probed with polyclonal AR antibodies (N-20; Santa Cruz Biotechnology), and blots were visualized by using peroxidase-conjugated second antibody and an ECL detection kit (Amersham Pharmacia Biosciences).

Morphologic Classification of Growing Follicles. Sections were taken at intervals of 30 μm, and 6-μm paraffin-embedded sections were mounted on slides. Routine hematoxylin and eosin staining was performed for histologic examination by light microscopy. Follicle numbers in 12 sections per ovary were evaluated as primary follicles (oocyte surrounded by a single layer of cuboidal granulosa cells), preantral follicles (oocyte surrounded by two or

Conflict of interest statement: No conflicts declared.

This paper was submitted directly (Track II) to the PNAS office.

Abbreviations: AR, androgen receptor; DHT, 5α-dihydrotestosterone; POF, premature ovarian failure.

‡H.S. and T.M. contributed equally to this work.

**To whom correspondence should be addressed. E-mail: uskato@mail.ecc.u-tokyo.ac.jp.

www.pnas.org/cgi/doi/10.1073/pnas.0506736102

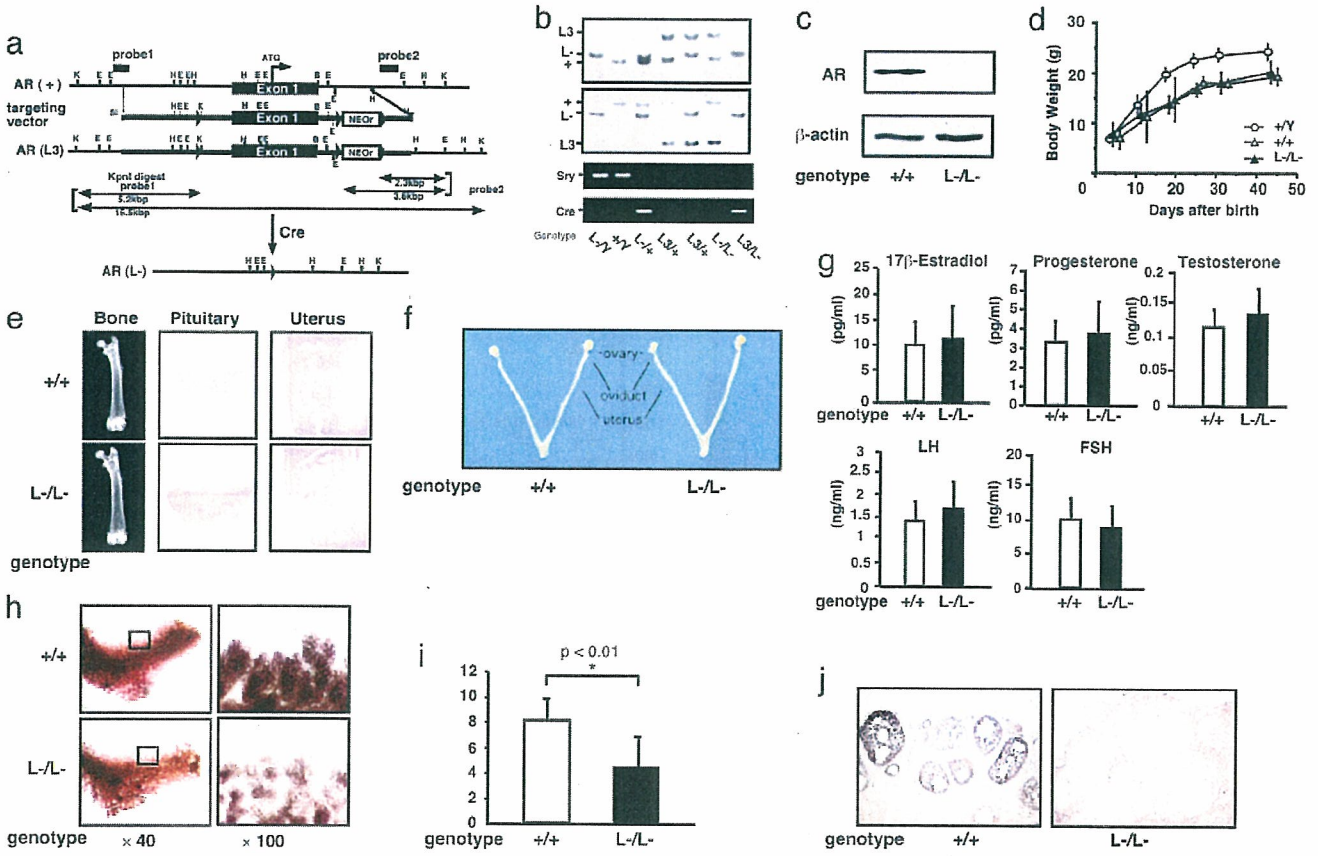

Fig. 1. Phenotypic characterization of AR knockout female mice. (*a*) Diagram of the wild-type *Ar* genomic locus (+), floxed *AR* L3 allele (L3), and *AR* allele (L-) obtained after Cre-mediated excision of exon 1. K, KpnI; E, EcoRI; H, HindIII; B, BamHI. LoxP sites are indicated by arrowheads. The targeting vector consisted of a 7.6-kb 5′ homologous region containing exon 1, a 1.3-kb 3′ homologous region, a single loxP site, and the neo cassette with two loxP sites. (*b*) Detection of the Y chromosome-specific *Sry* gene in $AR^{-/Y}$ mice by PCR. (*c*) Absence of AR protein in $AR^{-/-}$ mice ovaries by Western blot analysis using a specific C-terminal antibody. (*d*) Normal weight gain in $AR^{-/-}$ females. (*e*) Histology of pituitary, uterus, and bone tissues in $AR^{-/+}$ and $AR^{-/-}$ females at 8 weeks of age. (*f*) Female reproductive organs were macroscopically normal in $AR^{-/-}$ mice. (*g*) Serum hormone levels at the proestrus stage in $AR^{-/-}$ mice were not significantly altered. Serum 17β-estradiol, progesterone, testosterone, luteinizing hormone (LH), and follicle-stimulating hormone (FSH) levels in $AR^{+/+}$ (n = 13) and $AR^{-/-}$ (n = 10) females at 8–10 weeks of age are shown. (*h*) Lobuloalveolar development is impaired in $AR^{-/-}$ mammary glands. Whole mount of inguinal mammary glands (*Left*) and its higher magnification (*Right*) were prepared on day 3 of lactation. (*i*) Average number of pups per litter is markedly reduced in $AR^{-/-}$ mice at 8 weeks of age. Data are shown as mean ± SEM and analyzed by using Student's t test. (*j*) AR immunocytochemistry in $AR^{+/-}$ and $AR^{-/-}$ ovaries. Sections were counterstained with eosin.

more layers of granulosa cells with no antrum), or antral follicles (antrum within the granulosa cell layers enclosing the oocyte). Follicles were determined to be atretic if they displayed two or more of the following criteria within a single cross section: more than two pyknotic nuclei, granulosa cells within the antral cavity, granulosa cells pulling away from the basement membrane, or uneven granulosa cell layers (15).

Immunohistochemistry. Sections were subjected to a microwave antigen retrieval technique by boiling in 10 mM citrate buffer (pH 6.0) in a microwave oven for 30 min (16). The cooled sections were incubated in 1% H_2O_2 for 30 min to quench endogenous peroxidase and then incubated with 1% Triton X-100 in PBS for 10 min. To block nonspecific antibody binding, sections were incubated in normal goat serum for 1 h at 4°C. Sections were then incubated with anti-AR (1:100) or anti-cleaved caspase-3 (1:100) in 3% BSA overnight at 4°C. Negative controls were incubated in 3% BSA without primary antibody. The ABC method was used to visualize signals according to the manufacturer's instructions. Sections were incubated in biotinylated goat anti-rabbit IgG (1:200 dilution) for 2 h at room temperature, washed with PBS, and incubated in avidin–biotin–horseradish peroxidase for 1 h. After thorough washing in PBS, sections were developed with 3,3′-diaminobendizine tetrahydrochloride substrate, slightly counterstained with eosin, dehydrated through an ethanol series and xylene, and mounted.

Estrus Cycles and Fertility Test. To determine the stage of the estrus cycle (proestrus, estrus, and diestrus), vaginal smears were taken every morning and stained with Giemsa solution. For evaluation of female fertility for 15 weeks, an 8- or 24-week-old wild-type or $AR^{-/-}$ female was mated with a wild-type fertile male, replaced every 2 weeks with the other fertile male. Cages were monitored daily and for an additional 23 days, and the presence of seminal plugs and number of litters were recorded.

RNA Extraction and Quantitative Competitive RT-PCR. Total ovarian RNA was extracted by using TRIzol (Invitrogen) (16). Oligo-dT-primed cDNA was synthesized from 1 μg of ovarian RNA by using SuperScript reverse transcriptase (Gibco BRL, Gaithersburg, MD) in a 20-μl reaction volume, 1 μl of which was then diluted serially (2- to 128-fold) and used to PCR-amplify an internal control gene, *cycA*, to allow concentration estimation.

PHYSIOLOGY

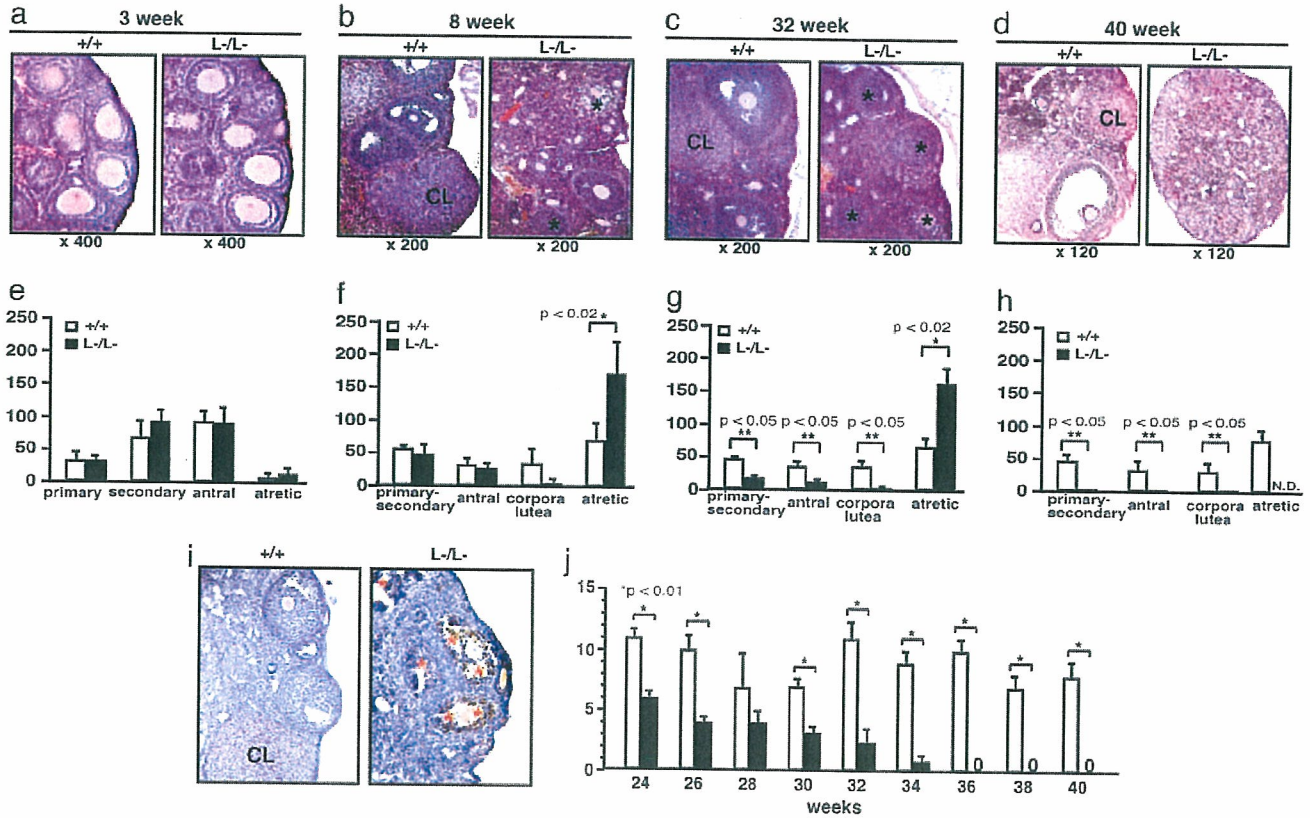

Fig. 2. POF in $AR^{-/-}$ female mice. (*a–d*) Histology of $AR^{+/+}$ and $AR^{-/-}$ ovaries at 3 weeks, 8 weeks, 32 weeks, and 40 weeks of age. All sections were stained with hematoxylin and eosin. An asterisk marks the atretic follicle. CL, corpus luteum. (*e–h*) Relative follicle counts at 3 weeks (*e*), 8 weeks (*f*), 32 weeks (*g*), and 40 weeks (*h*) of age. Numbers represent total counts of every fifth section from serially sectioned ovaries ($n = 4$ animals per genotype). (*i*) Immunohistochemical study for activated, cleaved caspase-3 revealed increased positive cells (apoptotic cells) in $AR^{-/-}$ ovaries. Sections were counterstained with hematoxylin. An asterisk marks the caspase-3-positive cell. CL, corpus luteum. (*j*) Age-dependent reduction in the number of pups per litter in $AR^{-/-}$ female mice. A continuous breeding assay was started at 24 weeks of age ($n = 6–10$ animals per genotype). For all panels, data are shown as mean ± SEM and were analyzed by using Student's *t* test.

Primers were designed from cDNA sequences of *Kitl* (M57647; nucleotides 1099–1751), Gdf9 (NM008110; nucleotides 720-1532), *Bmp15* (NM009757; nucleotides 146–973), *Ers2* (NM010157; nucleotides 1139–1921), *Pgr* (NM008829; nucleotides 1587–2425), *Cyp11a1* (NM019779; nucleotides 761-1697), *Cyp17al* (M64863; nucleotides 522–932), *Cyp19* (D00659; nucleotides 699-1049), *Fshr* (AF095642; nucleotides 625-1427), *Lhr* (M81310; nucleotides 592-1331), *Ptgs2* (AF338730; nucleotides 3–605), and *Ccnd2* (NM009829; nucleotides 150-1065) and chosen from different exons to avoid amplification from genomic DNA.

GeneChip Analysis. Ovaries were isolated and stabilized in RNA-*later* RNA Stabilization Reagent (Ambion, Austin, TX) before RNA purification (17). Total RNA was purified by using an RNeasy mini kit (Qiagen, Valencia, CA) according to the manufacturer's instructions. First-strand cDNA was synthesized from 5 μg of RNA by using 200 units of SuperScript II reverse transcriptase (Invitrogen, Carlsbad, CA), 100 pmol T7-$(dT)_{24}$ primer [5′-GGCCAGTGAATTGTAATACGACTCAC-TATAGGGAGGCGG-$(dT)_{24}$-3′], 1× first-strand buffer, and 0.5 mM dNTPs at 42°C for 1 h. Second-strand synthesis was performed by incubating first-strand cDNA with 10 units of *Escherichia coli* ligase (Invitrogen), 40 units of DNA polymerase I (Invitrogen), 2 units of RNase H (Invitrogen), 1× reaction buffer, and 0.2 mM dNTPs at 16°C for 2 h, followed by 10 units of T4 DNA polymerase (Invitrogen) and incubation for another 5 min at 16°C. Double-stranded cDNA was purified by using GeneChip Sample Cleanup Module (Affymetrix, Santa Clara, CA) according to the manufacturer's instructions and labeled by *in vitro* transcription by using a BioArray HighYield RNA transcript labeling kit (Enzo Diagnostics, Farmingdale, NY). Briefly, dsDNA was mixed with 1× HY reaction buffer, 1× biotin-labeled ribonucleotides (NTPs with Bio-UTP and Bio-CTP), 1× DTT, 1× RNase inhibitor mix, and 1× T7 RNA polymerase and incubated at 37°C for 4 h. Labeled cRNA was then purified by using GeneChip Sample Cleanup Module and fragmented in 1× fragmentation buffer at 94°C for 35 min. For hybridization to the GeneChip Mouse Expression Array 430A or 430B or Mouse Genome 430 2.0 Array (Affymetrix), 15 μg of fragmented cRNA probe was incubated with 50 pM control oligonucleotide B2, 1× eukaryotic hybridization control, 0.1 mg/ml herring sperm DNA, 0.5 mg/ml acetylated BSA, and 1× hybridization buffer in a 45°C rotisserie oven for 16 h. Washing and staining were performed by using a GeneChip Fluidic Station (Affymetrix) according to the manufacturer's protocol. Phycoerythrin-stained arrays were scanned as digital image files and analyzed with GENECHIP OPERATING SOFTWARE (Affymetrix) (17).

Luciferase Assay. The *Kitl* promoter region (−2866 to −1 bp) was inserted into the pGL3-basic vector (Promega) for assay using the Luciferase Assay System (Promega) (14, 16). Cells at 40–50% confluence were transfected with a reference pRL-CMV

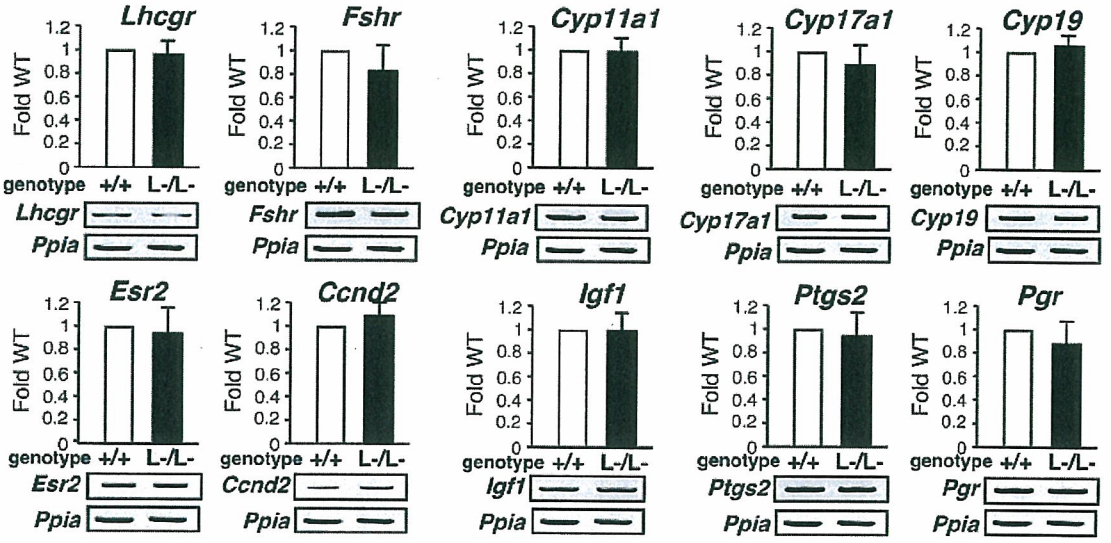

Fig. 3. No significant alterations in mRNA levels of several major regulators in folliculogenesis. Shown is semiquantitative RT-PCR of LH receptor (*Lhr*), FSH receptor (*Fshr*), p450 side chain cleavage enzyme (*Cyp11a1*), 17-α-hydroxylase (*Cyp17a1*), Aromatase (*Cyp19*), estrogen receptor-β (*Esr2*), cyclin D2 (*Ccnd2*), insulin-like growth factor 1 (*Igf1*), cyclooxygenase 2 (*Ptgs2*), or progesterone receptor (*Pgr*) gene expression in $AR^{+/+}$ and $AR^{-/-}$ ovaries. Results shown were representative (using one ovary per genotype in each experiment) of five independent experiments.

plasmid (Promega) using Lipofectamine reagent (GIBCO/BRL, Grand Island, NY) to normalize transfection. Results shown are representative of five independent experiments.

Results and Discussion

Subfertility of $AR^{-/-}$ Female Mice at 8 Weeks of Age. The *Ar* gene located on the X chromosome was disrupted in mice by using the Cre/Lox P system (6) (Fig. 1 *a–c*). Female $AR^{-/-}$ mice showed normal growth compared with the wild-type littermates (Fig. 1*d*), with no detectable bone loss (Fig. 1*e*) or obesity common for male $AR^{-/Y}$ mice (8, 9). Young (8-week-old) $AR^{-/-}$ females appeared indistinguishable from the wild-type littermates, displayed normal sexual behavior (7), and produced the first offspring of normal body size at the expected age. Macroscopic appearance of their reproductive organs, including uteri, oviducts, and ovaries, also appeared normal (Fig. 1*f*). Histological analysis showed no significant abnormality in the uterus or pituitary (Fig. 1*e*), whereas mammary ductal branching and elongation were substantially reduced, as revealed by whole-mount analysis (Fig. 1*h*). Serum levels of 17β-estradiol, progesterone, testosterone, luteinizing hormone, and follicle-stimulating hormone were also within normal range in 8-week-old mutant females at the proestrus stage (Fig. 1*g*), suggesting that the two-cell two-gonadotrophin system in female reproductive and endocrine organs (18) was intact in $AR^{-/-}$ mice at 8 weeks of age. The most obvious early sign of abnormal reproductive function in the $AR^{-/-}$ females was that their average numbers of pups per litter were only about half of those of the wild-type littermates, ($AR^{+/+}$, 8.3 ± 0.4 pups per litter; $AR^{-/-}$, 4.5 ± 0.5 pups per litter) (Fig. 1*i*).

$AR^{-/-}$ Female Mice Developed POF Phenotypes. Histological analysis of 8-week-old $AR^{-/-}$ ovaries clearly showed that numbers of atretic follicles were significantly increased, with decreased numbers of corpora lutea (Fig. 2 *b* and *f*). This finding suggests that the reduced pup numbers were due to impaired folliculogenesis in AR-deficient ovaries. Indeed, AR protein expression was readily detectable in the wild-type 8-week-old ovaries (Fig. 1*j*), with AR expressed at the highest levels in growing follicle granulosa cells at all developmental stages and at relatively low levels in corpora lutea. Thus, AR appears to play a regulatory role in granulosa cells during their maturation to the luteal phase.

To investigate this possibility, we examined the ovarian phenotype of female $AR^{-/-}$ mice at different ages. At 3 weeks, ovaries contain various stages of follicles, including primary, secondary, and antral follicles in wild-type animals (Fig. 2*a*) (19). In $AR^{-/-}$ ovaries at 3 weeks of age, the folliculogenesis appeared to be unaltered, with normal numbers and localization of primary and secondary follicles (Fig. 2 *a* and *e*). However, degenerated folliculogenesis became evident with further aging. Although follicles and corpora lutea at all developmental stages were still present, corpora lutea numbers were clearly reduced in 8-week-old $AR^{-/-}$ mutants (Fig. 2 *b* and *f*), similar to that observed in another mouse line (20). Expected apoptosis was seen in atretic follicles by activated caspase-3 immunohistochemistry assays (Fig. 2*i*). But, by 32 weeks of age, defects in folliculogenesis in $AR^{-/-}$ ovaries became profound, with fewer follicles observed and increased atretic follicles (Fig. 2 *c* and *g*), and >40% (5 of 12 mice) of the $AR^{-/-}$ females were already infertile. By 40 weeks, all $AR^{-/-}$ females became infertile, with no follicles remaining (Fig. 2 *d* and *h*); at the same age, $AR^{+/+}$ females were fertile and had normal follicle numbers. Consistent with progressive deficiency in folliculogenesis, the pup number per litter steadily decreased in aging $AR^{-/-}$ females (Fig. 2*i*). These data indicate that AR plays an important physiological role at the preluteal phase of folliculogenesis.

Alteration in Gene Expressions of Several Major Regulators Involved in the Oocyte–Granulosa Cell Regulatory Loop. To explore the molecular basis underlying the impaired folliculogenesis in $AR^{-/-}$ ovaries, we analyzed expression of several major known regulators and markers of folliculogenesis (21–23). Surprisingly, no significant alterations in mRNA levels of LH receptor (*Lhr*), FSH receptor (*Fshr*), p450 side chain cleavage enzyme (*Cyp11a1*), 17-α-hydroxylase (*Cyp17a1*), aromatase (*Cyp19*), estrogen receptor-β (*Esr2*), cyclin D2 (*Ccnd2*), or insulin-like growth factor 1 (*Igf1*) of 8-week-old $AR^{-/-}$ ovaries at the proestrus stage, and further cyclooxygenase 2 (*Ptgs2*) or progesterone receptor (*Pgr*) at the estrus stage, were detected by

PHYSIOLOGY

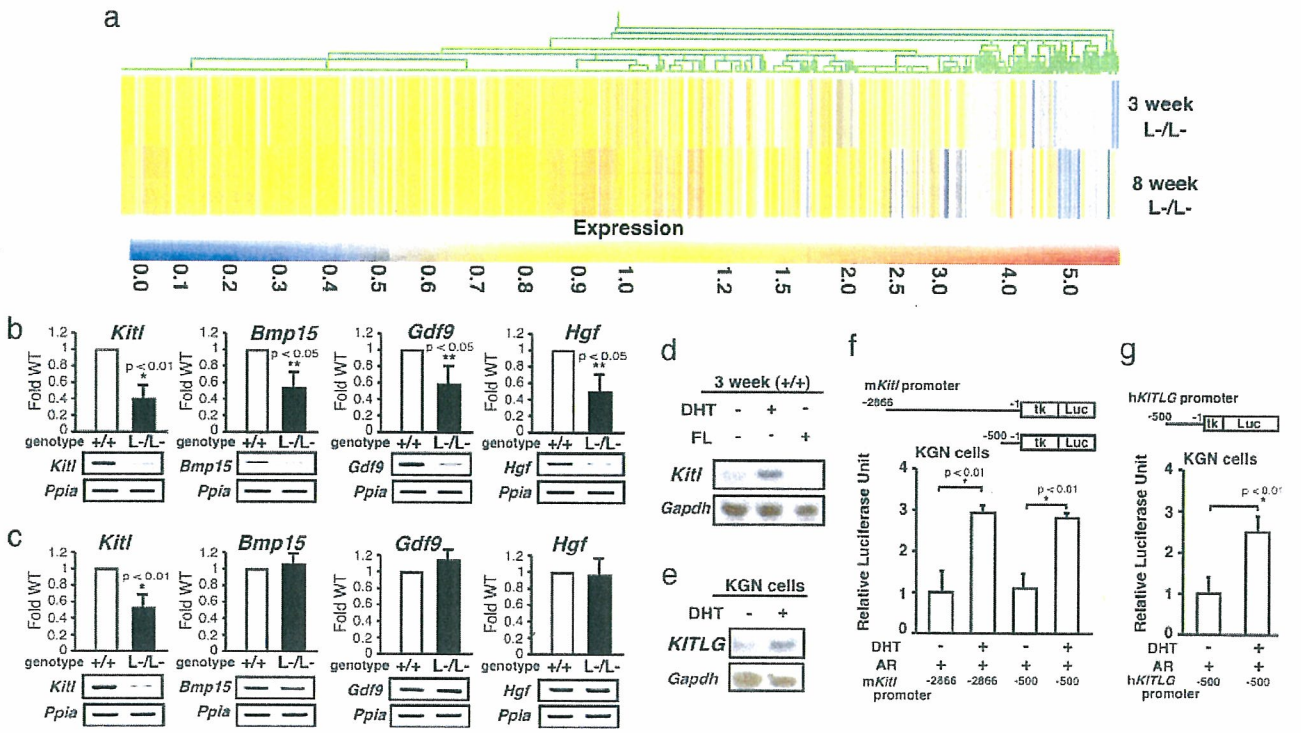

Fig. 4. Genome-wide microarray analysis and semiquantitative RT-PCR revealed that expression of the oocyte–granulosa cell regulator loop was down-regulated in $AR^{-/-}$ ovaries. (*a*) Microarray analysis of $AR^{-/-}$ compared with $AR^{+/+}$ ovaries at 3 and 8 weeks of age. Data obtained from microarray analysis as described in *Materials and Methods* were used to generate a cluster analysis. Each vertical line represents a single gene. The ratios of gene expression levels in $AR^{-/-}$ ovaries compared with wild type are presented. (*b* and *c*) Semiquantitative RT-PCR analysis of AR-regulated genes identified from the microarray study. Results shown are representative (using one ovary per genotype in each experiment) of five independent experiments. Data are shown as mean ± SEM and were analyzed by using Student's *t* test. (*d*) Comparison of *Kitl* gene expression by Northern blot analysis among placebo-, DHT-, and flutamide (FL)-treated $AR^{+/+}$ mouse ovaries. (*e*) Induction of *KITLG* gene expression by DHT treatment in KGN cells. (*f* and *g*) Androgen responsiveness in the mouse and human *kit ligand* promoters by a luciferase assay performed by using KGN cells. Data are shown as mean ± SEM and were analyzed by using Student's *t* test.

semiquantitative RT-PCR analysis (Fig. 3). Genome-wide microarray analysis (17) of RNA from 8-week-old $AR^{-/-}$ ovaries at the proestrus stage has been undertaken to identify AR-regulated genes. In comparison with $AR^{+/+}$ ovaries, expressions of 772 genes were down-regulated, whereas 351 genes were up-regulated in $AR^{-/-}$ ovaries (Fig. 4*a*; see also Tables 1 and 2, which are published as supporting information on the PNAS web site). Several genes known to be involved in the oocyte–granulosa cell regulatory loop (24) were identified as candidate AR target genes, including KIT ligand (*Kitl*) (25), morphogenetic protein 15 (*Bmp15*) (26), growth differentiation factor-9 (*Gdf9*) (27), and hepatocyte growth factor (*Hgf*) (28). Impaired folliculogenesis had been reported in mice deficient in each of these three regulators (26, 27, 29). To validate the microarray data, we performed semiquantitative RT-PCR analysis of 8-week-old $AR^{-/-}$ ovary RNA and confirmed that expression of these factors was down-regulated (Fig. 4*b*). To identify a regulator downstream of the AR signaling at an earlier stage of folliculogenesis, 3-week-old $AR^{-/-}$ ovaries that, as pointed out earlier, display no apparent phenotypic abnormality were examined. Fewer genes had altered expression levels (519 genes up-regulated; 326 genes down-regulated) (Fig. 4*a*; see also Tables 3 and 4, which are published as supporting information on the PNAS web site), and, of the four regulators tested by RT-PCR, only *Kitl* was found to be down-regulated at this age (Fig. 4*c*). Because *Kitl* is a granulosa cell-derived factor and stimulates oocyte growth and maturation (29–31), down-regulation of the *Kitl* expression in 3-week-old or even younger $AR^{-/-}$ ovaries may trigger impairment in folliculogenesis at a later age. To test for possible *Kitl* gene regulation by AR, 3-week-old wild-type females were treated with 5α-dihydrotestosterone (DHT). At 4 h after hormone injection, a clear induction of *Kitl* expression was observed in the ovaries, whereas a known antiandrogen flutamide attenuated the induction by DHT (Fig. 4*d*). The induction of endogenous human *kit ligand* (*KITLG*) gene by DHT was also observed in human granulosa-like tumor cells (KGN) in culture (Fig. 4*e*). Furthermore, androgen-induced transactivation of mouse and human *kit ligand* promoters (32) was observed by a luciferase reporter assay (33) in KGN (Fig. 4 *f* and *g*), 293T, and HeLa (data not shown) cells. However, no response to DHT was detected in the similar assay using promoters of the *Bmp15*, *Gdf9*, and *Hgf* genes (data not shown). Thus, we have shown that, in a regulatory cascade controlling folliculogenesis, *Kitl* represents a direct downstream target of androgen signaling.

As an upstream regulator, AR may also be indirectly involved in control of expression of other genes critical for folliculogenesis, because an age-dependent down-regulation of *Bmp15*, *Gdf9*, and *Hgf* gene expression was also observed in $AR^{-/-}$ ovaries. *Bmp15* and *Gdf9* are oocyte-derived factors that promote the development of surrounding granulosa cells in growing follicles (34, 35), whereas *Hgf* is secreted by theca cells and acts as a granulosa cell growth factor (36). Down-regulation of these factors, presumably due to decreased *Kitl* expression, may lead to impaired bidirectional communication between oocyte and granulosa cells (24) and, eventually, to early termination of folliculogenesis, as in POF syndrome.

Thus, we have identified AR as a novel regulator of follicu-

logenesis that apparently acts in the regulatory cascade upstream of the major factors controlling ovarian function, confirming the previous findings of the AR expression in granulose cells of growing follicles (3). Although not immediately relevant to the ovarian physiology, abnormal development of the mammary glands observed in our AR-deficient mice adds further strong evidence of an essential role of the AR not only in male, but also in female, reproductive function.

With increasing age of the first childbirth by women in the modern society, POF syndrome has become an important social and medical problem. Our findings suggest that POF syndrome may be caused by an impairment in androgen signaling and that X chromosomal mutations affecting the *AR* gene function may play a key role in hereditary POF. From clinical perspective, the present study provides evidence that AR can be a beneficial therapeutic target in treatment of POF syndrome patients.

We thank T. Iwamori and H. Tojo for expert advice on mammary gland anatomy, Y. Kanai for ovarian phenotypic analysis, members of the KO project team at the laboratory of Nuclear Signaling (Institute of Molecular and Cellular Biosciences) for their support, A. P. Kouzmenko for helpful suggestions, and H. Higuchi for manuscript preparation. This work was supported in part by the Program for Promotion of Basic Research Activities for Innovative Biosciences and priority areas from the Ministry of Education, Culture, Sports, Science, and Technology (to S.K.).

1. Laml, T., Preyer, O., Umek, W., Hengstschlager, M. & Hanzal, H. (2002) *Hum. Reprod. Update* **8,** 483–491.
2. Davison, R. M., Davis, C. J. & Conway, G. S. (1999) *Clin. Endocrinol. (Oxford)* **51,** 673–679.
3. Tetsuka, M., Whitelaw, P. F., Bremner, W. J., Millar, M. R., Smyth, C. D. & Hillier, S. G. (1995) *J. Endocrinol.* **145,** 535–543.
4. Ehrmann, D. A., Barnes, R. B. & Rosenfield, R. L. (1995) *Endocr. Rev.* **16,** 322–353.
5. Norman, R. J. (2002) *Mol. Cell. Endocrinol.* **191,** 113–119.
6. Kato, S. (2002) *Clin. Pediatr. Endocrinol.* **11,** 1–7.
7. Sato, T., Matsumoto, T., Kawano, H., Watanabe, T., Uematsu, Y., Sekine, K., Fukuda, T., Aihara, K., Krust, A., Yamada, T., *et al.* (2004) *Proc. Natl. Acad. Sci. USA* **101,** 1673–1678.
8. Sato, T., Matsumoto, T., Yamada, T., Watanabe, T., Kawano, H. & Kato, S. (2003) *Biochem. Biophys. Res. Commun.* **300,** 167–171.
9. Kawano, H., Sato, T., Yamada, T., Matsumoto, T., Sekine, K., Watanabe, T., Nakamura, T., Fukuda, T., Yoshimura, K., Yoshizawa, T., *et al.* (2003) *Proc. Natl. Acad. Sci. USA* **100,** 9416–9421.
10. Li, M., Indra, A. K., Warot, X., Brocard, J., Messaddeq, N., Kato, S., Metzger, D. & Chambon, P. (2000) *Nature* **407,** 633–636.
11. Sekine, K., Ohuchi, H., Fujiwara, M., Yamasaki, M., Yoshizawa, T., Sato, T., Yagishita, N., Matsui, D., Koga, Y., Itoh, N. & Kato, S. (1999) *Nat. Genet.* **21,** 138–141.
12. Yoshizawa, T., Handa, Y., Uematsu, Y., Takeda, S., Sekine, K., Yoshihara, Y., Kawakami, T., Arioka, K., Sato, H., Uchiyama, Y., *et al.* (1997) *Nat. Genet.* **16,** 391–396.
13. Gubbay, J., Collignon, J., Koopman, P., Capel, B., Economou, A., Munsterberg, A., Vivian, N., Goodfellow, P. & Lovell-Badge, R. (1990) *Nature* **346,** 245–250.
14. Yanagisawa, J., Yanagi, Y., Masuhiro, Y., Suzawa, M., Watanabe, M., Kashiwagi, K., Toriyabe, T., Kawabata, M., Miyazono, K. & Kato, S. (1999) *Science* **283,** 1317–1321.
15. Britt, K. L., Drummond, A. E., Cox, V. A., Dyson, M., Wreford, N. G., Jones, M. E., Simpson, E. R. & Findlay, J. K. (2000) *Endocrinology* **141,** 2614–2623.
16. Ohtake, F., Takeyama, K., Matsumoto, T., Kitagawa, H., Yamamoto, Y., Nohara, K., Tohyama, C., Krust, A., Mimura, J., Chambon, P., *et al.* (2003) *Nature* **423,** 545–550.
17. Fujimoto, N., Igarashi, K., Kanno, J., Honda, H. & Inoue, T. (2004) *J. Steroid Biochem. Mol. Biol.* **91,** 121–129.
18. Couse, J. F. & Korach, K. S. (1999) *Endocr. Rev.* **20,** 358–417.
19. Elvin, J. A. & Matzuk, M. M. (1998) *Rev. Reprod.* **3,** 183–195.
20. Hu, Y. C., Wang, P. H., Yeh, S., Wang, R. S., Xie, C., Xu, Q., Zhou, X., Chao, H. T., Tsai, M. Y. & Chang, C. (2004) *Proc. Natl. Acad. Sci. USA* **101,** 11209–11214.
21. Elvin, J. A., Yan, C., Wang, P., Nishimori, K. & Matzuk, M. M. (1999) *Mol. Endocrinol.* **13,** 1018–1034.
22. Zhou, J., Kumar, T. R., Matzuk, M. M. & Bondy, C. (1997) *Mol. Endocrinol.* **11,** 1924–1933.
23. Burns, K. H., Yan, C., Kumar, T. R. & Matzuk, M. M. (2001) *Endocrinology* **142,** 2742–2751.
24. Matzuk, M. M., Burns, K. H., Viveiros, M. M. & Eppig, J. J. (2002) *Science* **296,** 2178–2180.
25. Joyce, I. M., Pendola, F. L., Wigglesworth, K. & Eppig, J. J. (1999) *Dev. Biol.* **214,** 342–353.
26. Yan, C., Wang, P., DeMayo, J., DeMayo, F. J., Elvin, J. A., Carino, C., Prasad, S. V., Skinner, S. S., Dunbar, B. S., Dube, J. L., *et al.* (2001) *Mol. Endocrinol.* **15,** 854–866.
27. Dong, J., Albertini, D. F., Nishimori, K., Kumar, T. R., Lu, N. & Matzuk, M. M. (1996) *Nature* **383,** 531–535.
28. Parrott, J. A., Vigne, J. L., Chu, B. Z. & Skinner, M. K. (1994) *Endocrinology* **135,** 569–575.
29. Driancourt, M. A., Reynaud, K., Cortvrindt, R. & Smitz, J. (2000) *Rev. Reprod.* **5,** 143–152.
30. Huang, E. J., Manova, K., Packer, A. I., Sanchez, S., Bachvarova, R. F. & Besmer, P. (1993) *Dev. Biol.* **157,** 100–109.
31. Packer, A. I., Hsu, Y. C., Besmer, P. & Bachvarova, R. F. (1994) *Dev. Biol.* **161,** 194–205.
32. Grimaldi, P., Capolunghi, F., Geremia, R. & Rossi, P. (2003) *Biol. Reprod.* **69,** 1979–1988.
33. Kitagawa, H., Fujiki, R., Yoshimura, K., Mezaki, Y., Uematsu, Y., Matsui, D., Ogawa, S., Unno, K., Okubo, M., Tokita, A., *et al.* (2003) *Cell* **113,** 905–917.
34. Otsuka, F. & Shimasaki, S. (2002) *Proc. Natl. Acad. Sci. USA* **99,** 8060–8065.
35. Joyce, I. M., Clark, A. T., Pendola, F. L. & Eppig, J. J. (2000) *Biol. Reprod.* **63,** 1669–1675.
36. Parrott, J. A. & Skinner, M. K. (1998) *Endocrinology* **139,** 2240–2245.

BMC Genomics

BioMed Central

Methodology article

Open Access

"Per cell" normalization method for mRNA measurement by quantitative PCR and microarrays

Jun Kanno*†[1], Ken-ichi Aisaki†[1], Katsuhide Igarashi[1], Noriyuki Nakatsu[1], Atsushi Ono[1], Yukio Kodama[1] and Taku Nagao[2]

Address: [1]Division of Cellular and Molecular Toxicology, National Institute of Health Sciences, 1-18-1, Kamiyoga, Setagaya-ku, Tokyo 158-8501, Japan and [2]President, National Institute of Health Sciences, 1-18-1, Kamiyoga, Setagaya-ku, Tokyo 158-8501, Japan

Email: Jun Kanno* - kanno@nihs.go.jp; Ken-ichi Aisaki - aisaki@nihs.go.jp; Katsuhide Igarashi - igarashi@nihs.go.jp; Noriyuki Nakatsu - n-nakatsu@nihs.go.jp; Atsushi Ono - Atsushi@nibio.go.jp; Yukio Kodama - kodama@nihs.go.jp; Taku Nagao - nagao@nihs.go.jp

* Corresponding author †Equal contributors

Published: 29 March 2006

*BMC Genomics*2006, **7**:64 doi:10.1186/1471-2164-7-64

Received: 06 November 2005
Accepted: 29 March 2006

This article is available from: http://www.biomedcentral.com/1471-2164/7/64

Abstract

Background: Transcriptome data from quantitative PCR (Q-PCR) and DNA microarrays are typically obtained from a fixed amount of RNA collected per sample. Therefore, variations in tissue cellularity and RNA yield across samples in an experimental series compromise accurate determination of the absolute level of each mRNA species per cell in any sample. Since mRNAs are copied from genomic DNA, the simplest way to express mRNA level would be as copy number per template DNA, or more practically, as copy number per cell.

Results: Here we report a method (designated the "Percellome" method) for normalizing the expression of mRNA values in biological samples. It provides a "per cell" readout in mRNA copy number and is applicable to both quantitative PCR (Q-PCR) and DNA microarray studies. The genomic DNA content of each sample homogenate was measured from a small aliquot to derive the number of cells in the sample. A cocktail of five external spike RNAs admixed in a dose-graded manner (dose-graded spike cocktail; GSC) was prepared and added to each homogenate in proportion to its DNA content. In this way, the spike mRNAs represented absolute copy numbers per cell in the sample. The signals from the five spike mRNAs were used as a dose-response standard curve for each sample, enabling us to convert all the signals measured to copy numbers per cell in an expression profile-independent manner. A series of samples was measured by Q-PCR and Affymetrix GeneChip microarrays using this Percellome method, and the results showed up to 90 % concordance.

Conclusion: Percellome data can be compared directly among samples and among different studies, and between different platforms, without further normalization. Therefore, "percellome" normalization can serve as a standard method for exchanging and comparing data across different platforms and among different laboratories.

Background

Normalization of gene expression data between different samples generated in the same laboratory using a single platform, and/or generated in different geographical

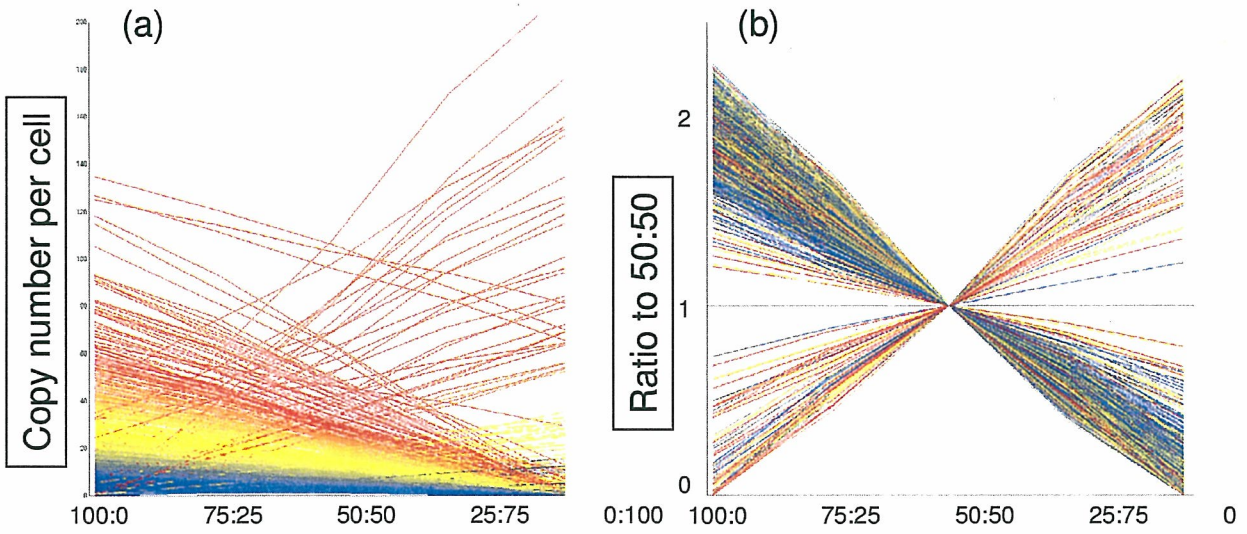

Figure 1
Dose-response linearity check by LBM. Dose-response linearity of the Affymetrix GeneChip by the LBM (liver-brain mix) sample set. Five samples, i.e. mixtures of mouse liver and brain at ratios of 100:0, 75:25, 50:50, 25:75 and 0:100, were spiked with GSC and measured by Affymetrix GeneChips Mouse430-2. Signals were normalized by the Percellome method as described in the text. Line graphs are in (a) copy numbers and (b) ratio to 50:50 sample for the top 1,000 probe sets with coefficient of correlation (R^2) closest to 1 among those having 1 copy or more per cell in the 50:50 sample (19,979 probe sets out of 45,101). The number of probe sets with $R^2 > 0.950$ was 8,655, and $R^2 > 0.900$ was 11,719.

regions using multiple platforms, is central to the establishment of a reliable reference database for toxicogenomics and pharmacogenomics. Transforming expression data into a "per cell" database is an effective way of normalizing expression data across samples and platforms. However, transcriptome data from the quantitative PCR (Q-PCR) and DNA microarray analyses currently deposited in the database are related to a fixed amount of RNA collected per sample. Variations in RNA yield across samples in an experimental series compromise accurate determination of the absolute level of each mRNA species per cell in any sample. Normalization against housekeeping genes for PCRs, and global normalization of ratiometric data for microarrays, is typically performed to account for this informational loss. Additional methods, such as the use of external mRNA spikes, reportedly improve the quality of data from microarray systems. For example, Holstege et al. [1] described a spike method against total RNA, based on their finding that the yields of total RNA from wild type and mutant cells were very similar. Hill et al. [2] reported a spike method against total RNA for normalizing hybridization data such that the sensitivities of individual arrays could be compared. Lee et al. [3] demonstrated that "housekeeping genes" cannot be used as a reference control, and van de Peppel et al. [4] described a normalization method of mRNA against total RNA using an external spike mixture. To achieve satisfactory performance they used multiple graded doses of external spikes, covering a wide range of expression, in order to align the ratiometric data by Lowess normalization [5]. Hekstra et al. [6] presented a method for calculating the final cRNA concentration in a hybridization solution. Sterrenburg et al. [7] and Dudley et al. [8] reported the use of common reference control samples for two-color microarray analyses of the human and yeast genomes, respectively. These are pools of antisense oligo sequences against all sense oligos present on the microarray. Instead of antisense oligos, Talaat et al. [9] used genomic DNA as a common reference control in studies of *E. coli*. Statistical approaches have been proposed for ratiometric data to improve inter-microarray variations, especially of non-linear relations [10]. However, because control samples may differ among studies, ratiometric data cannot easily be compared across multiple studies unless a common reference, such as a mixture of all antisense counterparts of spotted sense sequences is used [7-9]. Nevertheless, as long as the normalization is calibrated to total RNA, variations in total RNA profile cannot be effectively cancelled out. Although

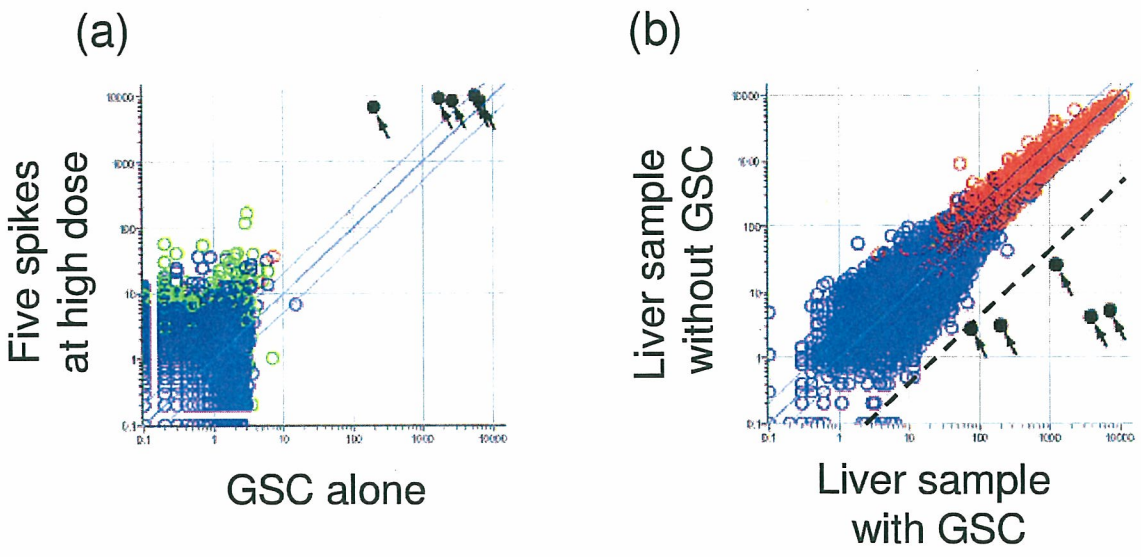

Figure 2
Cross-hybridization of GSC. Cross-hybridization of the GSC spike mRNAs to Affymetrix GeneChip. (a) A scatter plot of a blank sample with the GSC (horizontal axis) and a blank with the five spike RNAs at a high dosage (vertical axis) measured by MG-U74v2A GeneChips (raw values generated by Affymetrix MAS 5.0 software). The five spikes are indicated by black dots with arrows. Signals of the murine probe sets were below 20 on the horizontal axis, indicating negligible cross-hybridization of GSC spike mRNAs to the murine probe sets. (b) A scatter plot of a liver sample with GSC (horizontal axis) and without GSC (vertical axis) measured by MG-U74v2A GeneChips. The five spikes are again indicated by black dots with arrows. The dotted line is the 1/25 fold (4%) line. Cross-hybridization of mouse liver mRNAs to the GSC signals was considered negligible (less than 4%).

some of these reports share the idea that "absolute expression" and "transcripts per cell" should entail robust normalization, further practical development to enable universal application has been awaited.

Here, we report a method for normalizing expression data across samples and methods to the cell number of each sample, using the DNA content as indicator. This normalization method is independent of the gene expression profile of the sample, and may contribute to transcriptome studies as a common standard for data comparison and interchange.

Results

Dose-response linearity of the measurement system as a basis for the Percellome method

The fidelity of transcript detection is the key to this "per cell" based normalization method, which generates transcriptome data in "mRNA copy numbers per cell". The Q-PCR system was tested by serially diluting samples to confirm the linear relationship between Ct values and the log of sample mRNA concentration (data not shown). High density oligonucleotide microarrays from Affymetrix [11] were used in our experiments. We tested the linearity of the Affymetrix GeneChips using a set of five samples made of mixtures of liver and brain in ratios of 100:0, 75:25, 50:50, 25:75, and 0:100 (designated "LBM" for liver-brain mix). The results showed a linear relationship ($R^2 > 0.90$) between fluorescence intensity and input for a sufficient proportion of probe sets, i.e. about 37% of the probe sets in the older MG-U74v2 and 70% in the newest Mouse Genome 430 2.0 GeneChip were above the detection level (approximately one copy per cell) in the 50:50 sample (Figure 1) [see Additional files 1 and 2].

Dose-response linearity alone is not sufficient to generate true mRNA copy numbers. An important additional requirement is that the ratio of signal intensity to mRNA copy number should be equal among all GeneChip probe sets of mRNAs and PCR primers. The Q-PCR primer sets were designed to perform at similar amplification rates to minimize differences between amplicons. The melting

Table 1: The spike factors for various organs/tissues

Species	Organ/Tissue (adult, unless otherwise noted)	Spike Factor	total RNA/genomic DNA	SD
Mouse	Liver	0.2	211	46
Mouse	Lung	0.02	22	4
Mouse	Heart	0.05	-	-
Mouse	Thymus	0.01	8	2
Mouse	Colon Epitherium	0.05	105	30
Mouse	Kidney	0.1	-	-
Mouse	Brain	0.1	-	-
Mouse	Suprachiasmatic nucleus (SCN)	0.1	-	-
Mouse	Hypothalamus	0.1	63	4
Mouse	Pituitary	0.1	52	8
Mouse	Ovary	0.02	35	4
Mouse	Uterus	0.02	42	12
Mouse	Vagina	0.02	81	38
Mouse	Testis	0.15	56	7
Mouse	Epididymis	0.07	53	16
Mouse	Bone marrow	0.02	14	3
Mouse	Spleen	0.02	-	-
Mouse	Whole Embryo	0.15	97	36
Mouse	Fetal Telencephalon E10.5–16.5	0.1	48	9
Mouse	Neurosphere (E11.5–14.5)	0.03	42	10
Mouse	E9.5 embryo heart	0.15	58	15
Mouse	cell lines	0.2	-	-
Rat	Liver	0.2	-	-
Rat	Kidney	0.2	-	-
Rat	Uterus	0.04	56	5
Rat	Ovary	0.04	56	9
Human	Cancer Cell Lines	0.2	116	26
Xenopus	liver	0.03	-	-
Xenopus	embryo	0.15	-	-

temperature was set between 60° and 65°C with a product size of approximately 100 base pairs using an algorithm (nearest neighbor method, TAKARA BIO Inc., Japan), and the amplification co-efficiency (E) was set within the range 0.9 ± 0.1 (E = 2^{-(1/slope)}-1 on a plot of log2 (template) against Ct value). For the GeneChip system, the signal/copy performance of each probe set depended on the strategy of designing the probes to keep the hybridization constant/melting temperature within a narrow range, ensuring that the dose-response performances of the probe sets were similar (cf. http://www.affymetrix.com/technology/design/index.affx). Failing this, any differences should at least be kept constant within the same make/version of the GeneChip. Taking into consideration the biases that lead to imperfections in estimating absolute copy numbers in each gene/probe set, we developed normalization methods to set up a common scale for Q-PCR and Affymetrix GeneChip systems.

The grade-dosed spike cocktail (GSC) and the "spike factor" for the Percellome method

A set of external spike mRNAs was used to transfer the measurement of cell number in the sample (as reflected by its DNA content) to transcriptome analysis. For the spikes, we utilized five *Bacillus subtilis* mRNAs that were left open for users in the Affymetrix GeneChip series. The extent to which the *Bacillus* RNAs cross-hybridized with other probe sets was checked for the Affymetrix GeneChip system. The GSC was applied to Murine Genome U74Av2 Array (MG-U74v2) GeneChips with or without a liver sample. As shown in Figure 2, cross-hybridization between *Bacillus* RNAs and the murine gene probe sets was negligible [see Additional files 3 and 4]. Mouse Genome 430 2.0 Array (Mouse430-2), Mouse Expression Arrays 430A (MOE430A) and B (MOE430B), Rat Expression Array 230A (RAE230A), *Xenopus laevis* Genome Array and Human Genome U95Av2 (HG-U95Av2) and U133A (HG-U133A) Arrays sharing the same probe sets for these spike mRNAs showed no sign of cross-hybridization with the *Bacillus* probes (data not shown).

We prepared a cocktail containing in vitro transcribed Bacillus mRNAs in threefold concentration steps, i.e. 777.6 pM (for AFFX-ThrX-3_at), 259.4 pM (for AFFX-LysX-3_at), 86.4 pM (for AFFX-PheX-3_at), 28.8 pM (for AFFX-DapX-3_at) and 9.6 pM (for AFFX-TrpnX-3_at). By referring to the amount of DNA in a diploid cell and employing a "spike factor" determined by the ratio of

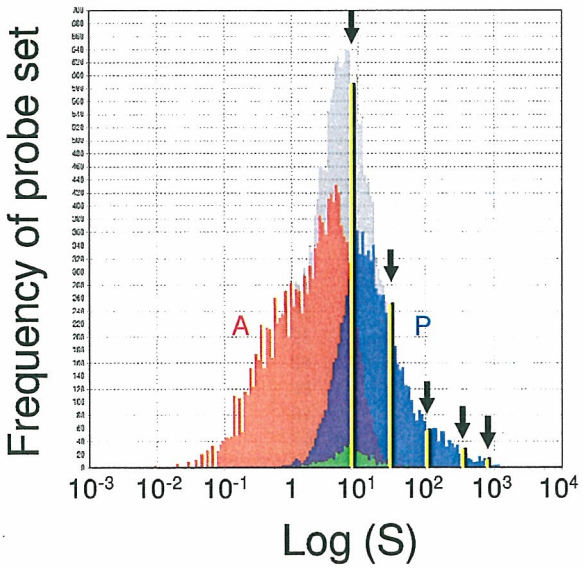

Figure 3
Positioning of GSC spike mRNAs in Affymetrix GeneChip dose-response range. A frequency histogram of the probe sets of Affymetrix GeneChip Mouse430-2 is shown. The histogram for all probe sets (gray) shows near-normal distribution. Blue columns are the "present" calls (P), red columns "absent" calls (A) and green "marginal" calls. The five yellow lines indicate the positions of the GSC spike mRNAs that are chosen to cover the "present" call range by a proper "spike factor".

total RNA to genomic DNA in a tissue type (Table 1), the spike mRNAs were calculated to correspond to 468.1, 156.0, 52.0, 17.3 and 5.8 copies per cell (diploid), respectively, for the mouse liver samples (spike factor = 0.2). The ratio of mRNAs in the cocktail is empirically chosen depending on the linear range of the measurement system and the available number of spikes. Here, we set the ratio to three to cover the "present" call probe sets of the Affymetrix GeneChip system (Figure 3).

We tested this grade-dosed spike cocktail (GSC) by Q-PCR and confirmed that the Ct values of the spike mRNAs were linearly related to the log concentrations (cf. Figure 4a), i.e. could be expressed as

$$Ct = \alpha \log C + \beta \quad \{1\}$$

The GSC was also tested by the GeneChip system and it was confirmed that the log of the spike mRNA signal intensities was linearly related to the log of their concentrations (cf. Figure 4b),

$$\log S = \gamma \log C + \delta \quad \{2\}$$

The linear relationship between the Ct values (Ct) and the log of RNA concentration (log C) was reasonable given the definition of Ct values (derived from the number of PCR cycles, i.e. doubling processes). The linear relationship between the log of GeneChip signal intensity (log S) and the log of RNA concentration (log C) was rationalized by the near-normal distribution of log S over all transcripts (cf. Figure 3).

Calculation of copy numbers of all genes/probe sets per cell

As described above, using a combination of DNA content and the spike factor of the sample, the GSC spike mRNAs become direct indicators of the copy numbers (C') per cell. When the samples were measured by Q-PCR or GeneChip analysis, the five GSC spike signals in each sample should obey function {1} for Q-PCR and function {2} for GeneChip with a good linearity. If the observed linearity was poor, a series of quality controls was performed and the measurement repeated. The coefficients of the functions were determined for each sample by the least squares method. Under the assumption that all genes/probe sets share the same signal/copy relationship, signal data for all genes/probe sets were fitted to the functions {1'} or {2'}, which are the individualized functions of {1} and {2} for each sample measurement (i).

$$Ct = \alpha i \log(C') + \beta i \quad \{1'\}$$

$$\text{Log } (S) = \gamma i \log(C') + \delta i \quad \{2'\}$$

(i = sample measurement no.)

The Q-PCR Ct values (Ct) and microarray signal values (S) of all mRNA species in the sample (i) are converted to copy numbers per cell (C') by the inverses of functions {1'} and {2'}, i.e. {3} and {4} below:

$$C' = B^{((Ct-\beta i)/\alpha i)} \quad \{3\}$$

for Q-PCR (Figure 4a).;

$$C' = B^{((\log S-\gamma i)/\delta i)} \quad \{4\}$$

for GeneChips (Figure 4b),

where B is the logarithmic base used in {1} and {2} (see Materials and Methods for details).

Real world performance of the Percellome method

The correspondence between Q-PCR and GeneChip was tested using a sample set from 2,3,7,8-tetrachlorodibenzodioxin (TCDD)-treated mice. Sixty male C57BL/6 mice

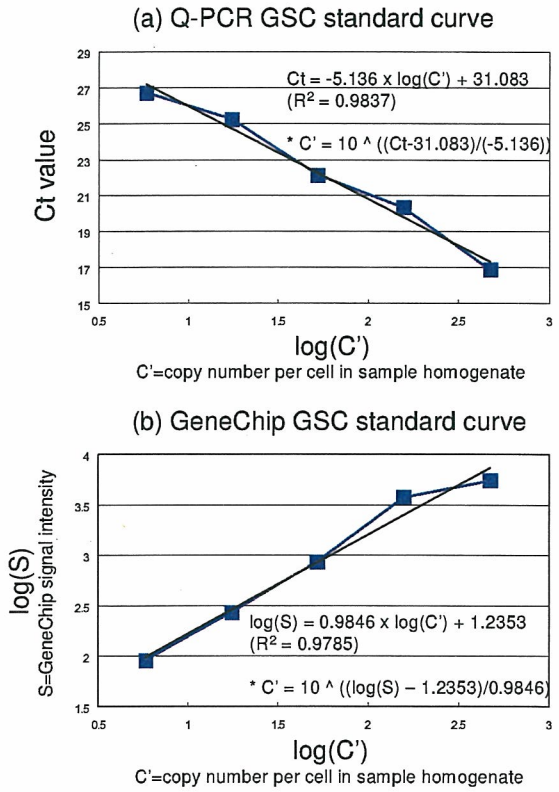

Figure 4
The dose-response linearity of the GSC spikes in Q-PCR and the Affymetrix GeneChip array system. Linear relationships are shown between (a) the Q-PCR Ct values and log of copy number (log (C')), and (b) the GeneChip log signal intensity (log(S)) and log of copy number (log (C')) of the GSC mRNAs. The regression functions were obtained by the least squares method. The inverse functions (*) were further used to generate the copy numbers of all other genes/probe sets for Percellome normalization.

were divided into 20 groups of 3 mice each. TCDD was administered once orally at doses of 0, 1, 3, 10 and 30 μg/kg, and the livers were sampled 2, 4, 8 and 24 h after administration. Nineteen primer pairs were prepared for Q-PCR and the Ct values of the liver transcriptome were measured. The same 60 liver samples were measured using the Affymetrix Mouse430-2 GeneChip [see Additional files 5 through 8 and 9 through 12]. Q-PCR and GeneChip data were normalized against cell number by functions {3} and {4}, respectively. The averages and standard deviations (sd) of each group (n = 3) were calculated and plotted as three layers of isoborograms on to 5 × 4 matrix three-dimensional graphs (Figure 5). Together with another sample set (data not shown), a total of thirty-six primer pairs were compared, and there was a correlation of up to 90% between the Q-PCR and GeneChip surfaces. It is notable that not only the average surfaces but also the +1sd and -1sd surfaces corresponded closely in shape and size. We infer that the differences resulted mainly from biological variations among the three animals in each experimental group rather than from measurement error (cf. Figure 7).

An important feature of Percellome normalization is its independence from the overall expression profile of the sample. When gene expression profiles differ among samples, Percellome normalization produces a robust transcriptome that is different from total-RNA dependent global normalization. As an example, Figure 6 shows the results of an experiment on the uterotrophic response of ovariectomized mice to estrogen treatment [12] [see Additional files 13 and 14]. The uteri of the vehicle control are atrophic because the ovaries, the source of intrinsic estrogens, are absent. The uteri of the treated groups are hypertrophic owing to estrogenic stimulus from the test compound administered. Global normalization (90 percentile) between the vehicle control group and the high-dose (1,000 mg/kg) group indicated that 4,600 of 12,000 probe sets showed 2-fold or greater increase, 470 were reduced by 0.5 or less, and 7,400 remained between these extremes. In contrast, analysis of Percellome-normalized data revealed that almost all the 12,000 probe sets showed a 2-fold or greater increase, including actin, GAPDH and other housekeeping genes. The hypertrophic tissues, consisting of cells with abundant cytoplasm, provide convincing evidence for the increases in various cellular components including housekeeping gene products.

Another important feature of Percellome normalization is the commonality of the expression scale across platforms. Batch conversion can be performed between results obtained from different platforms when the data are generated by the Percellome method. A practical strategy for such normalization is to prepare a set of samples from a target organ of interest with differences in gene expression, and measure them once by each platform. Data conversion functions with good linear dose-response relationships can be obtained individually for those genes/probe sets that are measured by both platforms (Figure 7).

Discussion

We have developed a novel method for normalizing mRNA expression values to sample cell numbers by adding external spike mRNAs to the sample in proportion to the genomic DNA concentration. For non-diploid or aneuploid samples, an average DNA content per cell should be determined beforehand for accurate adjustment. When there is significant DNA synthesis, a similar adjustment should be considered.

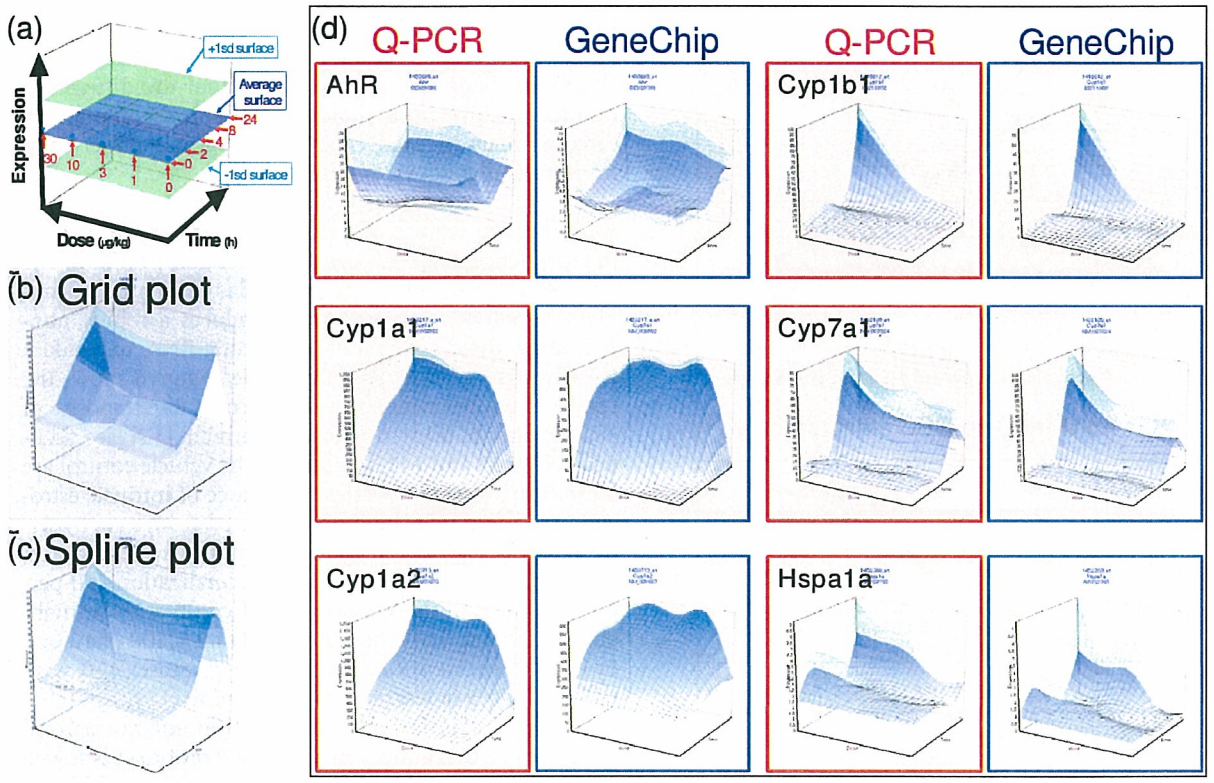

Figure 5

Correspondence between Q-PCR and GeneChip data. Sixty male C57BL/6 mice were divided into 20 groups of 3 mice each. 2,3,7,8-tetrachlorodibenzodioxin (TCDD) was administered once orally at doses of 0, 1, 3, 10 and 30μg/kg, and the liver was sampled 2, 4, 8 and 24 h after administration. The liver transcriptome was measured by the Affymetrix Mouse430-2 GeneChip. For Q-PCR, nineteen primary pairs were prepared and the Ct values of the same 60 liver samples were measured (19 genes and 5 spikes in duplicate, using a 96-well plate for 2 samples, total 30 plates). The Percellome data were plotted on to 3-dimensional graphs for average, +1sd, and – 1sd surfaces as shown in (a). The scale of expression (vertical axis) is the copy number per cell. The 0 h data (*) are copied from the 2 h/dose 0 point for better visualization of the changes after 2 h. The surfaces are demonstrated as a grid plot (b) where the grid points indicate one treatment group (n = 3), and a smoothened spline surface plot (c) for easier 3D recognition ((b), (c): Gys2 (glycogen synthase 2, 1424815_ at) showing a typical circadian pattern. (d) the smoothened plots of 6 representative genes/ probe sets generated by Q-PCR (red) and GeneChip (blue). AhR (arylhydrocarbon receptor, 1450695_at) showed imperfect correspondence. Cyp1a1 (cytochrome P450, family 1, subfamily a, polypeptide 1, 1422217_a_at) and Cyp1a2 (1450715_at) showed good correlations between Q-PCR and GeneChip except for the saturation in GeneChips above c. 400 copies per cell. Cyp1b1 (1416612_at) and Cyp7a1 (1422100_at) showed good correspondence. Hspa1a (heat shock protein 1A, 1452888_at) showed fair correspondence despite low copy numbers, near the nominal detection limit of the Affymetrix GeneChip system.

The smallest sample to which we have successfully applied the direct DNA quantification method with sufficient reproducibility is the 6.75 dpc (days post coitus) mouse embryo which consists of approximately 5,000 cells. This sample size is also approximately the lower limit for double amplification protocol to obtain sufficient amount of RNA for Affymetrix GeneChip measurement (cf. http://www.affymetrix.com/Auth/support/downloads/manuals/expression_print_manual.zip.)

High-resolution technology such as laser-capture microdissection (LCM) has become popular and the average sample size analyzed is getting smaller. An alternative method for LCM samples is to count the cell number in the course of microdissection. Although we have not yet applied Percellome method to LCM samples, we have applied the alternative method to cell culture samples to gain Percellome data. Stereological and statistical calculations should become available to correct the number of partially sectioned cells in the LCM samples. Another issue for small samples is the yield of RNA. Approximately

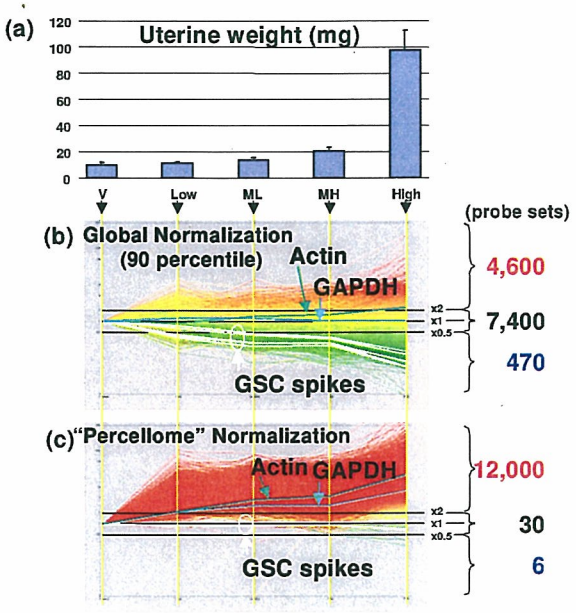

Figure 6
Uterotrophic response of ovariectomized female mice by an estrogenic test compound.(a) Shows the uterine weight, which increases in a dose-dependent manner; V, vehicle control; Low, low dose; ML, medium-low dose; MH, medium-high dose; High, high dose group. (b) Shows the line display of uterine gene expression (Affymetrix MG-U74v2 A GeneChips) normalized by global normalization (90 percentile), and (c) by the Percellome normalization. Averages of three samples per group were visualized (by K. A.). The five white lines are the GSC mRNAs. The green and blue lines are actin (AFFX-b-ActinMur/M12481_3_at) and GAPDH (glyceraldehyde-3-phosphate dehydrogenase, AFFX-GapdhMur/M32599_3_at), respectively. By global normalization, 7,400 probe sets remained unchanged and 4,600 probe sets increased more than two-fold in the H group compared to the V group, whereas almost all probe sets measured had increased. It is noted that housekeeping genes such as actin and GAPDH are significantly induced on a per cell basis.

30 ng of total RNA is retrieved from a single 6.75 dpc mouse embryo. This amount is sufficient for a double amplification protocol (DA) to prepare enough RNA for an Affymetrix GeneChip measurement. An inherent problem with the DA data is that the gene expression profile differs from that of the default single amplification protocol (SA). Consequently the DA percellome data differ from that of SA as if they were produced by a different platform. To bridge the difference, we applied the procedure that was used for data conversion between Q-PCR and GeneChip (cf. Figure 7). A set of spiked-in standard samples including the LBM sample set (of sufficient concentration) were measured by the SA protocol and diluted versions to the limit measured by the DA protocol. These data provided us with information about whether DA was successful as a whole (by comparing 5' signal to 3' signals of selected probe sets) and which probe sets were properly amplified by DA (by checking the linearity of the diluted LBM data). For those probe sets that proved to be linearly amplified, conversion functions between DA and SA were generated. These details, along with embryo expression data will be published elsewhere.

Figures 5 and 7 indicate a close correspondence between the data generated by Q-PCR and GeneChip analyses. Since each of the 60 samples was normalized individually against each GSC signal, the high similarity between the two platforms indicates the robustness and stability of this spike system (cf. Figure 7, Cyp7a1 data). Although more spikes could potentially increase the accuracy of normalization, our experience is that five spikes are practically sufficient for covering the detection range of GeneChip microarrays and Q-PCR, as long as they are used in combination with the "spike factor". The overall benefits of using a minimum number of external spikes include lower probability of cross-hybridization, a reduced number of wells and spots occupied by the spikes in the Q-PCR plates and small scale microarrays, and less effort in preparation, QC and supply.

The Percellome data can be truly absolute when all mRNA measurements including GSC spikes are strictly proportional to the original copy numbers in the sample homogenate. As noted earlier, this condition is not guaranteed by any platform despite linearity of response. Therefore, the Percellome-normalized values have some biases for each primer pair/probe set, depending on the steepness of the dose-response curves. An advantage of Percellome normalization is that, as long as such biases are consistently reproduced within a platform, the data can be compared directly among samples/studies on a common scale. Consequently, when a true value is obtained by any other measure, all the data obtained in the past can be simultaneously batch-converted to the true values.

This batch-conversion strategy can be extended to data conversion between different versions and different platforms, as long as the data are generated in copy numbers "per cell". We have shown an example between Affymetrix GeneChip and Q-PCR for limited numbers of probe sets (cf. Figure 7). Custom microarrays that accept our GSC for Percellome normalization are in preparation by Agilent Technologies (single color) and GE Healthcare (CodeLink Bioarray).